

**STUDY ON PREPARATION AND ELECTRICAL PROPERTIES OF  
CARBON COMPOSITE MULTIDIMENSIONAL MATERIALS**

多次元炭素複合材料の作製および電気特性に関する研究

**PENG BO**

**Supervisor: Prof. Masayoshi Fuji**

A Dissertation Submitted in Partial Fulfillment of the Requirements for the Degree of  
Doctor of Philosophy in Engineering in the Department of Frontier Materials



**NAGOYA INSTITUTE OF TECHNOLOGY**

**SEPTEMBER 2018**

© Copyright by PENG BO 2018

All Rights Reserved

## **ABSTRACT**

In order to fabricate carbon filled functional material with high dispersibility, electrical conductivity, and superior mechanical property, the multi-dimensional carbon composites were fabricated in this research. The fabricated carbon composites were formed as carbon nanoparticles/polymer 2D membranes, carbon nanoparticles/silica 3D ceramic bulk materials, as well as carbon nanotubes/silica 3D ceramic bulk materials. The variety of carbon composites were then studied their properties such as electrical conductivity and mechanical property. After that, the results were compared in order to investigate the effect of carbon material structures as well as carbon composites forms on their properties.

In Chapter 2, a micro-phase separation technique was chosen to fabricate carbon nanoparticles/polymer 2D membranes because it is one of the most common methods for preparation and production of a polymeric membrane. The micro-phase separation process studied here was in polymer system of cellulose acetate/acetone/water ternary solution. The carbon nanoparticles were added into the solution then the micro-phase separation occurred. After that, the carbon nanoparticles/polymer networks were heated so as to remove polymer from them. The carbon nanoparticles/polymer 2D membranes were further studied their electro-conductivity. The results revealed that the additional carbon nanoparticles in the ternary solution were provided network by the driving force of non-solvent, which is related to thermodynamic and compatible properties between particles and ternary solution. Meanwhile, the surface properties of nanoparticle had an effect on the binding force between neighboring particles as a result in the continued formation of a nanoparticle network structure. However, the membranes of carbon

nanoparticle membrane attached to glass substrate are quite lack of the possibility of independent existence. Which may possibly reduce their electrical property. To overcome such the problem, carbon materials in the next chapter were prepared without any glass substrate. Moreover, the other material used as a base matrix for carbon nanoparticles may provide higher mechanical properties than the glass substrate used.

Therefore, the silica ceramic was chosen to be a base matrix for carbon nanoparticles in the Chapter 3. In Chapter 3, the carbon nanoparticle/silica 3D ceramic composite matrixes were fabricated via non-firing process. The different volume percentages of carbon nanoparticles were added into silica ceramic in order to investigate the relationship between amount of carbon additive and the physical properties of the carbon nanoparticle/silica 3D ceramic composite matrixes including electro-resistivity and mechano-property. The results revealed that the highest amount of carbon in the carbon nanoparticles/silica to achieve solidified body percolates was 40 vol.%. According to the three-point bending tests, the carbon nanoparticle/silica 3D ceramic composite matrixes containing 20 vol.% carbon exhibited the highest strength as compared to other samples in this study. It can be inferred that the highest strength was possibly provided by the shrinkage prevention due to the aggregation of carbon nanoparticles leading to improve their mechanical property. However, the increased amount of carbon nanoparticles may break the bond between silica therefore the strength of those decreased. Moreover, the usage of a large amount of carbon used to form a network in ceramic matrixes is necessary for achieving a good electrical conductivity in the produced carbon nanoparticles/silica 3D ceramic composite matrixes of this chapter. Thus, carbon nanotubes (CNTs) have much attention to solve that problem because they have a better dispersibility than the carbon nanoparticles leading

to decrease the amount of carbon in ceramic matrixes. They also have a lower conductive percolation threshold to add into a ceramic matrix with the basis of ensuring mechanical strength for various applications.

In Chapter 4, CNTs/silica ceramic composite with electro-conductivity was fabricated and its application on electromagnetic field also discussed. Carbon composite ceramics have attracted much attention in the industry because of their excellent properties such as strong toughness, high electrical conductivity as well as low percolation threshold. Therefore, carbon nanotubes (CNTs) were used to incorporate silica ceramics in order to improve their electromagnetic properties. The number of CNTs in CNTs/silica composite ceramics was varied in order to investigate its effect on morphologies and electromagnetic properties of those. The composites were successfully fabricated by a non-firing process. The results revealed that the obtained CNTs/silica composite ceramic performed both electrical resistivity and bending strength. Meanwhile, the electromagnetic wave absorption ability achieved over a wide frequency. This indicates that the CNTs in CNTs/silica composite ceramics can be potentially applied as electromagnetic wave reflective material. This chapter not only proposed and realized the probability of a functional CNTs/silica ceramic material using a more facile and environmental method but the CNTs/ceramic composites also have perfect properties such as the mechanical strength and the dispersibility of CNTs fillers.

Chapter 5 introduced that CNTs/ceramic composites have attracted much attention for the industry because of their excellent properties. The additional interfacial bonding of silane functionalized multi-walled carbon nanotubes adding silica ceramic composites prepared by a non-firing process was therefore investigated in this work. MW-CNTs were previously oxidation treated by mixed acid for the further surface

modify with the participation of a silane 3-aminopropyl triethoxysilane (APTES), which improves the chemical bonding and dispersibility of CNTs in ceramic bodies. The existence of APTES chemical functionalization and mechanical property of CNTs/silica ceramic composites were investigated. Results showed the composites were easily prepared without calcining or sintering to form ceramic materials. They also showed that oxidation treatment introduced functional groups to CNTs surface for stable interfacial reacting with the amino groups on APTES. Obtained APTES-CNTs was sequentially combined with surface activated silica. This finding confirmed the improvements in dispersibility and enhanced mechanical property of composite material successfully.

Based on the above-mentioned studies, they can be concluded that our studies focused on investigating the ability of carbon materials filled multidimensionality (2D and 3D) functional nanocomposites. The ceramic materials prepared by the phase-separation process and an environmental friendly method known as the non-firing process can be potentially applied as electrical and EMI shielding materials. The different kinds of carbon materials having excellent conductive properties are added to the membrane polymer material and the bulk ceramic material so that the insulating material has electrical conductivity. The dispersibility and percolation threshold of carbon materials in the matrix materials were studied and finally applied to conductive composite materials and electromagnetic shielding materials. In recent years, most researchers believe that carbon nanotube-reinforced ceramic materials mainly depend on the dispersion of carbon nanotubes in the matrix, sufficient densification, and proper interfacial bonding between the carbon nanotubes and the matrix. In addition, it is also related to the number of carbon nanotubes added and the structural integrity.

## TABLE OF CONTENTS

<b>LIST OF FIGURES</b> .....	<b>V</b>
<b>LIST OF TABLES</b> .....	<b>VII</b>
<b>Chapter1 General Introduction</b> .....	<b>1</b>
1.1 Introduction of nano-ceramic materials.....	1
1.1.1 Preparation method of nano-ceramic materials .....	1
1.1.2 Functional nano-ceramic materials.....	3
1.1.3 Application of functional nano-ceramic materials .....	4
1.2 Introduction of carbon/ceramic composite materials. ....	5
1.2.1 Carbon black.....	5
1.2.2 Carbon nanotubes .....	6
1.2.3 Conclusion of carbon/ceramic composite materials.....	9
1.3 Conductive properties of carbon-doped composite materials. ....	10
1.3.1 Conductive Mechanism of carbon-doped composite material. ....	10
1.3.2 Effect of carbon-doped composite materials on conductive properties. ....	13
1.4 Object of the Thesis.....	16
1.5 Thesis Organization.....	17
References .....	19
<b>Chapter2 Micro-phase Separation Process to Prepare Carbon Nanoparticles</b> <b>Added Functional Polymer Membrane with Network Structure</b> .....	<b>27</b>
2.1 Introduction .....	27
2.2 Experimental Section.....	28
2.2.1 Materials .....	28

2.2.2 Preparation of ternary system membrane and carbon nanoparticle added membrane .....	29
2.2.3 Characterizations .....	30
2.3 Results and Discussion .....	30
2.3.1 Membrane of CA/Ace/W ternary system .....	30
2.3.2 Membrane of carbon nanoparticles added CA/Ace/W ternary system .....	33
2.3.3 Heat treatment and electro-conductivity of membrane .....	35
2.4 Conclusion .....	37
References .....	37
<b>Chapter 3 Preparation and Discussion on Carbon Nanoparticles/Silica Composite Ceramics Fabricated by Non-Firing Ceramic Process.....</b>	
<b>41</b>	
3.1 Introduction .....	41
3.2 Experimental section .....	41
3.2.1 Materials and preparation .....	41
3.2.2 Characterization.....	42
3.3 Illustration for measurement of electrical conductivity.....	43
3.4 Results and discussion .....	44
3.4.1 Morphology of carbon nanoparticle/silica ceramic composites .....	44
3.4.2 Electro-conductivity and bending strength.....	46
3.5 Conclusion .....	49
References .....	49
<b>Chapter4 Effect of CNTs on Morphology and Electromagnetic Properties of Non-firing CNTs/silica Composite Ceramics: Fabrication and Application .....</b>	
<b>51</b>	
4.1 Introduction .....	51

4.2 Experimental section .....	52
4.2.1 Materials and preparation .....	52
4.2.2 Characterization.....	54
4.3 Illustration and significance of non-firing ceramic process. ....	55
4.4 Results and discussion .....	56
4.4.1 Raman spectra.....	56
4.4.2 Morphology of composites.....	57
4.4.3 Electro and mechano properties. ....	60
4.4.4 EMI reflective ability.....	62
4.5 Conclusion .....	64
References .....	64

## **Chapter5 Effect of Silane Modification on CNTs/silica to Enhance Composites**

<b>Interfacial Property and Dispersibility.....</b>	<b>71</b>
5.1 Introduction .....	71
5.2 Experimental section .....	73
5.2.1 Materials .....	73
5.2.2 Preparation process.....	73
5.2.3 Characterizations .....	74
5.3 Results and discussion .....	75
5.3.1 Raman spectra.....	75
5.3.2 FT-IR spectrum.....	76
4.3.3 Composite morphologies from cross-section view .....	78
5.3.4 XPS and bending strength .....	80
5.3.5 Composite bending strength property.....	83

5.4 Conclusion .....	84
References .....	85
<b>Chapter6 General Conclusion .....</b>	<b>91</b>
<b>Research Activities.....</b>	<b>95</b>
<b>List of Publications .....</b>	<b>99</b>
<b>Acknowledgement.....</b>	<b>101</b>

## LIST OF FIGURES

Fig. 1.1 The Equivalent Circuit Model of Conductive Composite.....	12
Fig. 2.1. Illustration of process during non-solvent inducing micro phase separation...	31
Fig. 2.2. Optical microscope and SEM images of polymer membrane corresponding to CA/water ratios of P3N15, P4N14 and P5N13. ....	31
Fig. 2.3. Illustrate of the micro phase separation process of cellulose acetate/acetone/water ternary system. ....	33
Fig. 2.4. P3N15 optical microscope and scanning electron micrographs of membrane from carbon nanoparticle added CA/acetone/water solution corresponding to particle weight percent.....	34
Fig. 2.5. P3N15 SEM images of different weight percent (a) 8%, (b) 4% and (c) 2.7% at polygon edge in membrane from carbon nanoparticle added water included ternary system corresponding to particle. ....	35
Fig. 2.6. TG-DTA curve of cellulose acetate. ....	36
Fig. 2.7. Scanning electron micrographs of P3N15 solution ratio with 4wt.% carbon nanoparticle added membrane heated under (a)300 °C, (b)350 °C and (c)400 °C, respectively.....	37
Fig.3.1. SEM images of composites with different carbon nanoparticles volume percentage from 10% to 90%. ....	45
Fig. 3.2. The mechanical properties and mechanical properties of carbon nanoparticle/silica using non-firing process .....	48
Fig. 4.1. Brief diagrammatic for planetary ball mill process.....	55
Fig. 4.2. Theoretic illustration of the non-firing ceramics preparation process from raw	

individual ceramic particle to ceramic body.....	55
Fig. 4.3. Raman spectra of (a) raw carbon nanotubes and (b) silica-carbon nanotubes composite with 1.0 vol.% content of carbon nanotubes.....	56
Fig. 4.4. SEM images of composite with different carbon nanotubes volume percentages from cross-section view. (a) 0.125 vol.% (b) 0.25 vol.% (c) 0.5 vol.% and (d) 1.0 vol.% High magnification images of (e)(f) 1.0 vol.% .....	58
Fig. 4.5. TEM images of composite powders (a) combined structure between ..... silica particles (low magnification) (b) (high magnification) and (c) boundary between CNTs- SiO <sub>2</sub> particles (low magnification) and (d) (high magnification).....	59
Fig. 4.6. Mechano and electro properties of composites with different CNTs amounts.	61
Fig. 4.7. Schematic of free space method.....	62
Fig. 4.8. Electromagnetic wave reflective ratio of CNTs/ceramic nanocomposites with different CNTs amounts. ....	63
Fig. 5.1 Raman spectra and I <sub>G</sub> /I <sub>D</sub> intensity ratios of raw and acid treated MW-CNTs. .	75
Fig. 5.2. FT-IR spectrum of raw MW-CNTs, acid treated MW-CNTs and APTES functionalized MW-CNTs reacted with silica nanoparticles.....	77
Fig. 5.3 Typical Scanning electron microscopy images of the CNTs/ceramic composites from cross-section view under low magnification are shown in Fig. 5.3 (a) (c) and high magnification in (b) (d).....	79
Fig. 5.4. XPS spectra of silica-acid CNTs and silica-APTES-CNTs (a) totle of elements, (b) C1s, (c) O1s, (d) Si2p and (e) N1s spectra of silica-APTES-CNTs and Illustration of composite.....	80
Fig. 5.5. Bending strength of silica-acid CNTs abd silica-APTES-CNTs with different CNTs vol.%. ....	83

## LIST OF TABLES

Table 3.1	The surface-activated condition by planetary ball mill. ....	42
Table 3.2	Experimental conditions. ....	42
Table. 3.3	Mechanical and electrical properties of carbon nanoparticles/silica composites. ....	46
Table. 4.1.	Component Volume and volume fractions of CNTs/silica composites. ....	54
Table. 5.1.	XPS analysis summary results of MW-CNTs added silica ceramic with/without APTES functionalized. ....	81



## **Chapter1 General Introduction**

### **1.1 Introduction of nano-ceramic materials**

As in many areas of materials and a higher requirement of nano materials, nano-ceramic came into being a kind of widely used materials, it is hoped not only maintain the advantages of the ceramic ordinary ceramics, but also has the flexibility and workability similar metal [1-3]. Material scientist pointed out that nano-ceramics is a strategic way to solve the ceramic brittleness [4]. The reason why nanomaterial technology is used to improve the function of traditional ceramic materials is due to the unique characteristics of nano materials, which are not available in conventional materials or micron-scale materials. Such as sintering temperature, nano- $\text{Al}_2\text{O}_3$  (1200~1300°C) lower than the conventional crystal grain  $\text{Al}_2\text{O}_3$  (>1800°C) lower 600~700°C [5,6],  $\text{TiO}_2$  can be reduced 800°C [7]; When the SiC and  $\text{Si}_3\text{N}_4$  refined to the nano level produced Blue-shift and red-shift phenomena and very broad frequency absorption spectra; photocatalytic properties occur when  $\text{TiO}_2$  is refined to nanometer-sized particles [8,9]. With the continuous development of nano-materials and technologies, the performance of nano-ceramics is increasingly perfect, and its superiority will be fully reflected.

#### **1.1.1 Preparation method of nano-ceramic materials**

Preparation methods of nano-ceramic materials mainly include preparation of nano-powders, forming and sintering. The key to improving the quality of nano-ceramics has been to solve the agglomeration of nano powder, cracking of formed billets and grain growth during sintering. The special sintering method of nano-ceramics can control the size of the nano-ceramic crystal grains, so as to prevent the growth of

the nano-ceramics, which seriously affects the unique properties of the nano-ceramics. The following methods are mainly used [10].

a) Hot-press sintering and reaction hot-press sintering [11]. In this method, a certain external pressure is added at the same time as the sintering, and if the chemical reaction is accompanied during the sintering, the reaction is called hot-press sintering. The advantage lies in that the nano powders are integrated into the nano-ceramics to maintain complete densification and the particle size does not increase significantly. Therefore, the nanopowder is widely used in the sintering of nano ceramics, and the relative density of the sample can generally increased.

b) Hot isostatic pressing [12]. This is a method of forming and sintering at the same time. It is a new technology that combines the use of isothermal pressure isostatic pressing and high-temperature sintering. It can further increase the density of nano-ceramics and overcome the lack of lateral pressure and product density in ordinary hot pressing. Uneven defects.

c) Microwave sintering [13]. Using the dielectric loss of the material in the microwave electric field, the entire ceramic is heated to the sintering temperature to achieve a dandified rapid sintering technique. Significant features compared to conventional sintering are: changing the microstructure and macroscopic properties of the material; saving time and energy; rapidly increasing the temperature, preventing grain growth during sintering.

d) Non-firing process, an environmental friendly ceramic material fabrication method [14,15]. The non-firing process means treating surface of raw ceramic powder by mechanical planetary ball mill activation [16] and continuously dispersing powder in an alkaline solvent [17] to form precipitates and then eventually prepare ceramics

solidified body. In addition, the fabrication processes should proceed at a much lower temperature (80 °C) than the sintering method, so that it effectively achieves the effect of reducing cost and energy without requiring any other special sintering equipment.

#### 1.1.2 Functional nano-ceramic materials

Nanometer oxide powder is between the solid and the molecule size (1 to 100 nm) metastable intermediates. With the ultra-fine powder, the electronic structure and crystal structure of the surface change, resulting in a special effect that is not possessed by the bulk material or the conventional microparticles. Nano-ceramic powder materials have the following outstanding properties: 1) The nano ceramic material has a very small particle size, a large specific surface and a high chemical activity, which can reduce the sintering densification temperature of the material and save energy. Generally 400~600°C lower than engineering ceramics, and sintering does not need to add any additives; 2) The densification and homogenization of the material composition structure improve the performance of the ceramic material and improve the reliability of its application; 3) The composition and structure of the material can be controlled from the nano-material structure level (1 to 100 nm), which is conducive to the full play of the potential performance of the ceramic material, and makes it possible to design the nano-material structure and performance orientation; 4) Since the ceramic is sintered after raw material processing and forming, and the particle size of the ceramic powder determines the microstructure and macroscopic properties of the ceramic material, if the particles of the powder are uniformly deposited, the sintering shrinks uniformly and the crystal grains grow uniformly, The smaller the particles are, the less defects are produced and the higher the strength of the prepared material. 5) The characteristics of nanomaterials mainly lie in the mechanical properties, including the hardness, fracture

toughness, and low temperature ductility of nanoceramic materials, especially the hardness and strength are greatly improved at high temperature [18,19].

Nano-ceramic materials can be divided into two types according to their properties: Nanostructured ceramics, another type of Nano functional ceramics. The former is in the traditional ceramic powder by adding nano-particles, or nano-crystallizing the traditional ceramic powder, by controlling the solidification or crystal phase size and distribution in the sintering solidification, thus changing the microstructure of the ceramic to improve its mechanical properties. The obtained nano-ceramic materials have such mechanical properties as hardness, strength, plasticity, and toughness. The latter is a nano-ceramic material that has special functions through the addition of nano-phases or particles that have unique functions, or that itself cannot be fully exhibited at the conventional micron level. These special functions include acoustics, optics, and electricity, magnetics, biological activity, and the sensitivity of the environment. For nano functional ceramics, it is necessary to take into account certain mechanical properties on the basis of ensuring certain function.

### 1.1.3 Application of functional nano-ceramic materials

The quantum confinement effect is obtained by controlling the growth of nanocrystals. Thus, a ferroelectric body with a unique performance can be obtained, which can improve the electromechanical conversion and pyroelectric properties of the piezoelectric pyrolysis material. Utilizing the large specific surface area of ultrafine particles can produce a variety of sensors with temperature-sensitive, pressure-sensitive, gas-sensitive properties, and so on. The advantage is that only a small amount of ultrafine particles can play a greater role. Therefore, such nano-ceramic materials have important applications in high-pressure sodium lamps [20], multilayer capacitors [21],

microwave devices [22], and chemical sensors [23].

Organic and inorganic bactericidal nano-particles with functions of sterilization, disinfection, deodorization, mildew proofing and the like can be incorporated into ceramic materials to obtain functional ceramics having functions of sterilization, disinfection, deodorization, and mildew proofing, and can be used for manufacturing sanitary ware, table stones, glass, and so on. If such nanoparticles are super diphasic or super amphiphilic, their incorporation into ceramic materials will enable ceramic products to have a self-cleaning and anti-fog effect, and can be used for windows of special-purpose glass products, agricultural films, and military equipment.

Nano-materials are used in the surface treatment of ceramic products to make the surface properties of products have new functions. If a thin layer of nano  $\text{SiO}_2$  is sprayed on the surface of a ceramic product, its smoothness is doubled and the grade of the product is also improved a lot. The addition of nano-materials in ceramic glazes can greatly improve the surface finish and sintered glaze properties of ceramics.

Nano-ceramic materials applied in bioactive materials, petrochemical catalytically active carriers, light-enhancing materials and laser materials have been reported, and some have even been used in industrial production and daily life.

## **1.2 Introduction of carbon/ceramic composite materials.**

### **1.2.1 Carbon black**

Compared with other carbon material fillers, carbon black has the advantages of reinforcing the plastic rubber, controlling the amount of addition to obtain an arbitrary conductivity, and so on [24,25]. Therefore, it is currently widely used. In addition, its practical history is also the longest. Carbon black can be divided into several types according to different methods and raw materials. Conductive fillers are just a part of

them. Filled carbon black must have the following basic characteristics: 1) Highly developed structure; 2) Large surface area (multiple pores); 3) Capture of electrons with less impurities; 4) Better crystallization (graphitization).

### 1.2.2 Carbon nanotubes

In the year 1991, S. Iijima in the Japanese NEC laboratory found carbon nanotubes in a vacuum arc evaporation process for the preparation of fullerenes by graphite electrodes [26]. Since then, research on carbon nanotubes has been a frontier and hot topic in the field of new international materials. Carbon nanotubes (CNTs) consist of one layer, two or more layers of cylindrical graphene sheets, so there are single-walled carbon nanotubes (SW-CNTs) and multi-walled carbon nanotubes (MW-CNTs). The distance between the layers is 0.34 nm, which is equivalent to the gap between the layers of carbon atoms in the graphite or the radius of the carbon nanospheres. As a new type of quasi-one-dimensional functional material, CNTs has the characteristics of small diameter and large aspect ratio. Its tube wall thickness is only a few nanometers, the tube diameter is several to several tens of nanometers, and the axial length of the tube is micrometers. On the order of centimeters, it is 10 to 1000 times of the diameter. This unique structure enables CNTs to have excellent mechanical and electrical properties. The mechanical properties of CNTs exceed any previous material, the modulus of elasticity is extremely high, more than 1 TPa, the mass is 1/6 of the same volume of steel, the strength is 10 to 100 times that of steel, and in vacuum 2800 °C can still exist stably, the thermal conductivity is double that of diamond, and the current transmission capability is 100 times of copper wire. CNTs has a unique electronic energy band structure. Conductivity is related to its structure size. Different structures of CNTs can be metallic or semi-conductive. It is an ideal one-dimensional quantum wire [27], and

can be used as a field effect transistor, field Emission electron source and molecular switch, Scanning Tunneling Microscope (STM) tips; In addition, CNTs, also has hydrogen storage capacity, adsorption capacity and microwave absorption capacity, has great potential as hydrogen storage materials, catalyst carriers and wave absorbing materials. , It is expected to become an ideal reinforcement for advanced composite materials [28,29].

Difficulty in material preparation limits the research of carbon nanotube composites: The most important problem is the uniform dispersion of CNTs in the matrix; also due to many methods involved in the high temperature processing or Substances that react with CNTs, thus causing CNTs damage or destruction; CNTs production is low, the price is still a problem.

Discussing on the dispersion in base material, Carbon nanotubes have large specific surface area and high surface energy. Carbon nanotubes are strongly agglomerated with van der Waals forces. In particular, carbon nanotubes prepared by organic catalytic cracking method are often bent and twisted together. This phenomenon will be reduced. The aspect ratio of carbon nanotubes affects the reinforcing effect of carbon nanotube-reinforced composites. Therefore, how to introduce carbon nanotubes and evenly disperse them on the substrate is very critical. Carbon nanotubes are introduced in two ways: in-situ [30-32] and external mixing [33-44]. For the external mixing method, it can be separated as:

a) Physical dispersion: Physical dispersion refers to the use of physical forces to disperse carbon nanotubes, including ultrasonic, ball milling, grinding, high-speed shearing and so on [35-37].

b) Chemical dispersion: Chemical dispersion method refers to the use of

surfactants, surface modifiers or surface functionalization to change the surface energy of carbon nanotubes, increase their wetting or adhesion characteristics, and reduce their tendency to agglomerate in continuous solvents: 1) Acid treatment: The acid solution of concentrated  $\text{H}_2\text{SO}_4/\text{HNO}_3$  mixed solution can completely disperse the carbon nanotubes. The reason is that the carbon nanotubes will be shortened during the acid treatment and the hydrophilic functional groups such as hydroxyl functional groups will be increased [36]. If concentrated nitric acid is used, the length of the carbon nanotubes becomes shorter, the tube body becomes straighter, the wall has  $-\text{OH}$ ,  $=\text{C}-\text{O}$  and  $-\text{COOH}$  functional groups are adsorbed, and the carbon nanotubes are uniformly dispersed in the solution [38]. Shaffer et al. also found that acid oxidation of carbon nanotubes grown by catalytic cracking ( $\text{HNO}_3:\text{H}_2\text{SO}_4=1:3$ ) will increase the phenolic and hydroxyl functional groups on the surface of nanotubes. The presence of these functional groups can make carbon nanotubes. Stable dispersion in water at higher concentration [39]; 2) Adding a surfactant: Adding a surfactant such as Ethylenimine or sodium dodecylsulfate (SDS) can uniformly disperse the carbon nanotubes in an aqueous solution through the sol-aggregation process. Due to the electrostatic interactions between different components, carbon nanotubes coated with titanium oxide and aluminum oxide particles can be obtained [40]. Polyvinylamine and anionic citric acid are added as a dispersant in aqueous solution to modify the surface of carbon nanotubes. Then, after heat treatment in  $\text{NH}_3$ , the gold nanoparticles can be adsorbed and filled into the nanotubes on the surface and inside [41]. Adding 20 dmb % of the copolymer as a dispersant in the alcohol solution can successfully convert 1.0 wt. % multi-walled carbon Nanotubes spread evenly [42]. The addition of cetyltrimethylammonium bromide ( $\text{C}_{16}\text{TMAB}$ ) or polyacrylic acid (PAA) or  $\text{C}_{16}\text{EO}$  as

dispersants in water can uniformly disperse the carbon nanotubes, but it is impossible to obtain absolute uniformity [43]. The addition of (3-Aminopropyl) triethoxysilane (APTES) and cationic surfactant ammonium citrate can uniformly disperse carbon nanotubes in aqueous solution. The anionic and cationic surfactants are uniformly distributed in the form of nanoparticles adsorbed on the surface of carbon nanotubes; 3) The physical chemical dispersion method: This method is a combination of physical methods, such as ultrasonic method, ball milling method, and chemical methods, such as acid treatment, adding surfactants, and so on in order to achieve the purpose of more uniform dispersion of the nanotubes on the substrate. With the addition of surfactants in combination with ultrasonic oscillation and ball milling, carbon nanotubes can be more evenly distributed in nano WC/Co powders [44].

### 1.2.3 Conclusion of carbon/ceramic composite materials.

Carbon materials have excellent mechanical properties, electrical properties and thermal conductivity and other physical properties. The research of carbon composites has become an important direction and hotspot in the application of composite materials. The introduction of carbon materials to prepare composite ceramic materials is expected to further improve the mechanical properties of ceramic materials, and at the same time increase their functional properties, achieve structural and functional integration, and can modulate the performance of ceramic materials through the arrangement and content control of carbon nanotubes. The reinforcing effect of carbon material on the matrix of ceramic material mainly depends on the dispersion degree of carbon material on the matrix of ceramic material, the survival of carbon material in the microstructure, and the interface state of carbon and ceramic matrix. The research on the molding, characteristics, destruction and strengthening mechanism of carbon-reinforced ceramic

matrix composites on the nano scale will greatly enrich the research content of ceramic materials and lay a foundation for further broadening the application of ceramic materials as advanced materials.

### **1.3 Conductive properties of carbon-doped composite materials.**

#### 1.3.1 Conductive Mechanism of carbon-doped composite material.

The conductive mechanism of the conductive composite is very complex, mainly involving how the conductive pathway is formed and how the conductive pathway is formed [45]. It was found that the conductivity of the conductive composite increases with the increase of the content of the conductive filler. When the critical value is reached, the conductivity will be several orders of magnitude leap. This is because the conductive filler forms a three-dimensional conductive network in the matrix (conductive channel). Masaka [46] explained this phenomenon in detail. The interfacial effect between base material and conductive filler has a great influence on the formation of conductive channels in the system.

During the preparation of the composite material, the free surface of the conductive filler particles becomes a wet interface, forming a base-filler interface layer, and the system generates excess interface energy. As the conductive filler increases, the interface energy of the composite system increases continuously. When the interface of the system is surplus to a universal constant that is independent of the type of composite, the conductive particles begin to form conductive networks, conductive paths, and the macroscopically, the conductivity of the system increases dramatically.

After the conductive channels are formed, the carrier transport of the conductive fillers distributed in the base matrix determines the electrical conductivity of the material. At present, three conductive mechanisms are widely studied: percolation

theory, tunneling effect and field emission.

a) Percolation theory:

Percolation means that when the amount of conductive filler increases to a critical value, a three-dimensional conductive network is formed in the composite matrix, and the electrical conductivity suddenly increases. This critical value is called the percolation threshold, which is the minimum concentration of conductive filler required to form a continuous conductive network. A variety of mathematical models explain this phenomenon. At present, the most commonly used is the power law of exponents proposed by Kirkpat [47]. That is, when the filler concentration reaches the percolation threshold, the electrical conductivity and filler content have the following relationship:

$$\sigma = \sigma_0 (V - V_c)^t$$

$\sigma$ : Conductivity of composite system,

$\sigma_0$ : Electrical conductivity of conductive fillers,

$V$ : Volume fraction of conductive filler,

$V_c$ : Percolation threshold,

$t$ : Constant, related to the dimensions, dimensions, and morphology of the filler.

For two-dimensional fillers,  $t$  is 1~1. For ordinary three-dimensional systems,  $t$  is 1.5~1.6. This theory only applies to the sharp increase in conductivity near the interpretation threshold.

b) Tunnel effect:

When the amount of conductive filler is low, the composite system has a large spacing between conductive particles, and no conductive pathway has been formed in the microstructure of the mixture. At this time, the conductive phenomenon still exists, mainly because the thermal vibration electrons inside the composite system can migrate

between the conductive particles. . The conduction current is an exponential function of the gap width of the conductive particles. The tunneling effect only occurs between conductive particles with very close distances. There is no such current conduction behavior. between conductive particles with large gaps.

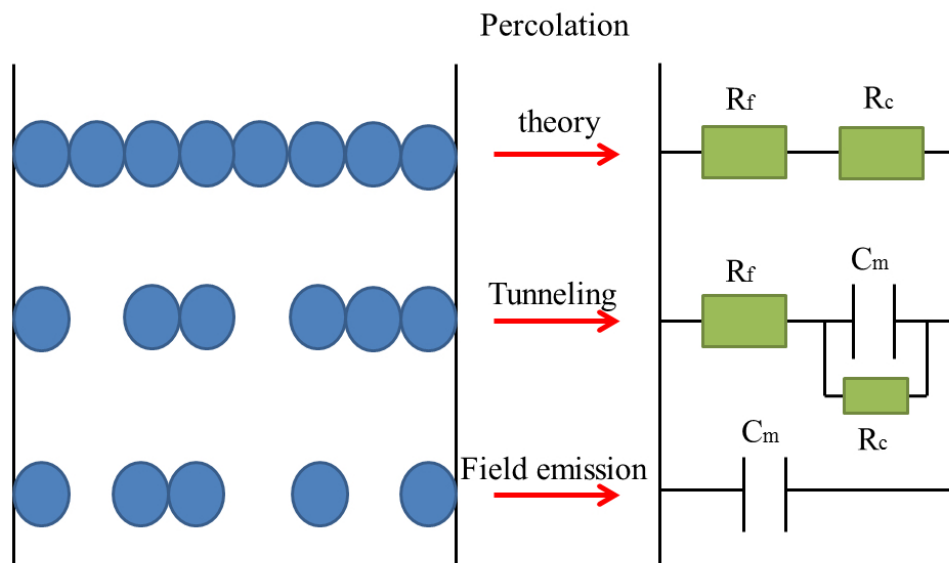


Fig. 1.1 The Equivalent Circuit Model of Conductive Composite

c) Field emission theory:

Van Beek [48] believe that when the content of conductive filler is small and the spacing between conductive particles is small and the electric field between the conductive particles is strong, electrons have a high probability to leap over the barrier layer of the interface layer and migrate to the adjacent conductive particles. Generate field emission current and conduct electricity. Due to the small influence of temperature and conductive filler concentration, it is universal. Fig. 1 is an equivalent circuit model of a conductive composite.

### 1.3.2 Effect of carbon-doped composite materials on conductive properties.

The carbon-doped composite material is a type of composite material in which a carbon material is dispersed into a matrix to improve its electrical conductivity through a certain processing method. The commonly used carbon-doped materials include carbon black, carbon nanotubes, and graphene.

#### a) Carbon black:

The carbon black can be uniformly dispersed into the matrix through a certain processing method to obtain a composite having certain conductivity. The main factors influencing the conductive properties of carbon black-doped composite are: carbon black type, filling amount, particle size, structure, and voidage; the structure, crystallinity, molecular weight, surface tension, and processing method of the matrix. A amount number of studies have shown that the smaller the diameter of the carbon black particles, the larger the surface area, the higher the degree of structural order, and the lower the voidage, the higher the electrical conductivity of the resulting composite system [58]. In addition, to obtain a highly conductive carbon black-doped composite, the carbon black doping concentration needs to be increased, but this will increase the melt viscosity and reduce the mechanical properties of the polymer [50].

#### b) Carbon nanotubes (CNTs):

Due to its high electrical conductivity and excellent mechanical properties, carbon nanotubes can be doped into a matrix as conductive filler, which not only improves the conductivity of the matrix but also improves the mechanical properties of the base material. Therefore, carbon nanotubes have become a hot spot as conductive fillers.

Carbon nanotubes are tubes formed by rolling a graphene sheet around a central axis with a certain degree of helix. The diameter of the carbon nanotubes is 1 nm to 100

nm, and the length of the carbon nanotubes can be in the order of microns or even centimeters. Due to the high aspect ratio, carbon nanotubes have extremely high mechanical strength and elastic modulus. In addition, carbon nanotubes also have good electrical properties and higher electrical conductivity than copper. These good properties make carbon nanotubes widely used to improve base material electrical properties. Currently used methods for preparing carbon nanotubes composites include solution mixing, melt blending, and in-situ polymerization. Carbon nanotubes have a higher aspect ratios comparing with carbon, Adohi [51] doped the multi-wall carbon nanotubes (MWCNT) and carbon black particles into the same polymer matrix by mechanical mixing. Study found that MWCNT doped polymers has a lower percolation threshold and is two orders of magnitude higher in conductivity than carbon black-doped composite. The carbon nanotube doped composite improves its conductive properties, first of all must have highly efficient conductive channels, and a good contact between individual carbon nanotubes; secondly, the contact resistance between individual carbon nanotubes also affects the system Conductive properties. Only when good electrical contact is established between each carbon nanotube can current be transmitted in the system [51]. Therefore, matrix type and preparation method of carbon nanotube-doped material, aspect ratio and degree of entanglement of carbon nanotubes, spatial distribution and degree of orientation of carbon nanotubes in matrix doped polymerization of carbon nanotubes The conductive properties of the material have a certain influence.

Currently studied conductive mechanisms are percolation theory, tunneling and field emission theory. The conductive properties of carbon-based materials doped composite are the result of competition between these three conductive mechanisms.

The introduction of carbon-based materials increases the conductivity of the base matrix by several orders of magnitude, mainly because conductive fillers form a conductive network in the matrix that provides a channel for carrier movement. In addition, the introduction of CNTs will also greatly improve the mechanical properties of the matrix. Compared with carbon black-doped composite material, CNT-doped material have lower percolation thresholds, the conductivity of the composite system can be significantly increased at lower conductive filler concentrations.

Although relevant research has made some progress, it still faces some challenges and is the direction of future development, such as: 1) How to improve the conductivity of carbon-doped materials doped composite material so that they can be applied to more fields. 2) How to improve the conductivity while making the composite system have high mechanical properties and other properties, namely the development of multi-functional carbon-based material doped composite material. 3) In the preparation process of carbon nanotubes, it is easy to generate entanglement to affect the conductive properties of the carbon nanotube-doped composite material, and how to make the carbon nanotubes have less entanglement and relatively uniform dispersion into the base to obtain better performance. 4) It is necessary to develop a graphene-based material that has few defects, a simple preparation method, a low cost, and a better doping of a base material.

With the deepening of research, carbon-based material doped composite material can be applied to a wider range of fields, because they not only have low-cost, conductive properties, but also have good flexibility for folding, will be in the field of a new generation of electronic devices Such as field effect transistors, solar cells, organic light-emitting diodes, energy storage devices, and electromagnetic shielding materials,

conductive coatings, and so on have attracted large amount of attention.

#### **1.4 Object of the Thesis**

Carbon materials have great application potential as reinforcing phase and conductive phase in the kinds of matrix such as polymer, ceramics, metals, and biology composite materials. Carbon materials are playing an increasingly important role in the preparation of composites with low density, high strength and other excellent electro and electromagnetic properties. On the ceramic matrix, a large number of studies have been discussed to add CNTs to Al or Si oxides. There have also been reports on the composite of CNTs with other oxides such as  $\text{TiO}_2$  and  $\text{V}_2\text{O}_5$ . However, there are still many problems to be solved in order to truly realize the practical application of composite materials, such as: characterize the microstructure and properties of composites and explain theoretically, solve the problem of dispersion and orientation of CNTs in the polymer matrix to ensure that a homogeneous composite material is obtained, and study the interaction mechanism with the matrix and the degree of interface binding. With the continuous deepening research on carbon material and the continuous advancement of related characterization techniques and manufacturing processes, these problems will be solved in the future, and carbon doped composite materials will be more widely used.

This thesis aims to investigate the ability of carbon materials filled different dimensionality (2D and 3D) functional nanocomposites prepared by phase-separation process and an environmental friendly ceramic material fabrication method named non-firing process to be applied as electrical and EMI shielding materials, in other words, different kinds of carbon materials having excellent conductive properties are added to the membrane polymer material and the bulk ceramic material so that the

insulating material has electrical conductivity. The dispersibility and percolation threshold of carbon materials in the matrix materials were studied and finally applied to conductive composite materials and electromagnetic shielding materials.

## **1.5 Thesis Organization**

The thesis consists of following 6 Chapters.

Chapter 1 is a general introduction to this thesis. The background of the research and the object of the work have been explained in detail.

In Chapter 2, electro-conductive 2D membranes material formed by carbon nanoparticle network array were fabricated via micro-phase separation process in the polymer system of cellulose acetate/acetone/water ternary solution. Micro-phase separation technique is the most common method for preparation and production of polymeric membrane. With the formation of polymer network, added nanoparticles became network by the drive of non-solvent owing to thermodynamic and compatible properties between particles and ternary solution. Meanwhile, the nanoparticle surface properties affected the binding force of neighbor particles for the continuous nanoparticle network structure. Heat treatment on the membrane aims at removing polymer from. Thus, electro-conductive nanoparticle network membrane can be facilely prepared.

In Chapter 3, carbon nanoparticle/silica 3D ceramic composite matrix was fabricated by non-firing process. To determine the relationship of carbon filler amount and the physical properties including electro-resistivity and mechano-property, different volume percentage of carbon nanoparticles were added into base silica ceramic of 10%, 20%, 30%, 40%, 50%, 60%, 70%, 80% and 90%. Results show that the carbon nanoparticles/silica solidified body percolates with 40 vol.% of filler. Also, from the

results of three-point bending test, the highest strength was at 20% of carbon nanoparticles. At this time, the strength was highest by preventing shrinkage as aggregate by carbon nanoparticles and making internal stress less likely to influence mechanical property. However, when increasing the amount of carbon nanoparticles to percolation concentration, the bond between silica was broken and the strength decreased.

In Chapter 4, it introduces 3D ceramic composite material filled by carbon nanotubes. Carbon composite ceramics have much attention for industry because of their excellent properties such as strong toughness, high electrical conductivity as well as low percolation threshold. Therefore, carbon nanotubes (CNTs) were used to incorporate with silica ceramics in order to improve their electromagnetic properties. The amount of CNTs in CNTs/silica composite ceramics was varied in order to investigate its effect on morphologies and electromagnetic properties of those. The composites were successfully fabricated by non-firing process. The results revealed that the obtained CNTs/silica composite ceramic have electrical resistivity and bending strength. At the same time, the electromagnetic wave absorption ability was discussed over a wide frequency. This indicates that the CNTs in CNTs/silica composite ceramics may be potentially applied for an electromagnetic wave reflective material.

In Chapter 5, multi-walled carbon nanotubes doped silica-base ceramic composite was investigated. CNTs/ceramic composites have much attention for the industry because of their excellent properties. The interfacial bonding of silane functionalized multi-walled carbon nanotubes adding silica ceramic composites by a non-firing process in this chapter. MW-CNTs were previously oxidation treated by mixed acid for the further surface modify with the participation of a silane 3-aminopropyl triethoxysilane

(APTES), which improves the chemical bonding and dispersibility of CNTs in ceramic bodies. The extent of APTES chemical functionalization and mechanical property of CNTs/silica ceramic composites were characterized using Raman spectrometer, FT-IR analysis, X-ray photoelectron spectroscopy (XPS), scanning electron microscopy (SEM) and three-point bending strength measurement. Results showed that composites were facilely prepared without calcining or sintering to form ceramic materials, and also showed that oxidization treatment introduced functional groups to CNTs surface for stable interfacial reacting with the amino groups on APTES. Obtained APTES-CNTs was sequentially combined with surface activated silica. This finding confirmed the improvements of dispersibility and enhanced mechanical property of composite material successfully.

In Chapter 6, a general conclusion of this work was made, and the purpose and method for the future exploration of related research are proposed.

## References

- [1] R.Z. Ma, J. Wu, B.Q. Wei, J. Liang, D.H. Wu, Processing and properties of carbon nanotubes–nano-SiC ceramic, *J. Mater. Sci.*, 33 (21)(1998) 5243-5246.
- [2] H.E. Mohammadloo, A.A. Sarabi, A.A.S. Alvani, H. Sameie, R. Salimi, Nano-ceramic hexafluorozirconic acid based conversion thin film: Surface characterization and electrochemical study, *Surf. Coat. Tech.*, 206 (19-20) (2012), 4132-4139.
- [3] H. Lv, S. Mu, Nano-ceramic support materials for low temperature fuel cell catalysts, *Nanoscale*, 6 (10)(2014) 5063-5074.
- [4] B.L. Hakim, S. Soepriyanto, A.A. Korda, B. Sunendar, The ceramic brittleness of the pressed and sintered yttria zirconia-mullite-magnesia system, *AIP*

- Conference Proceedings, 1677 (2015).
- [5] L. Gao, J.S. Hong, H. Miyamoto, S.D.D.L. Torre, Bending strength and microstructure of Al<sub>2</sub>O<sub>3</sub> ceramics densified by spark plasma sintering, *J. Euro. Ceram. Soc.*, 20(12)(2000) 2149-2152.
- [6] X. Qu, F. Wang, C. Shi, N. Zhao, E. Liu, C. He, F. He, In situ synthesis of a gamma-Al<sub>2</sub>O<sub>3</sub> whisker reinforced aluminum matrix composite by cold pressing and sintering, *Mater. Sci. Engin.: A*, 709 (2018) 223-231.
- [7] M. Jovani, M. Domingo, T. R. Machado, E. Longo, H. Beltrán-Mir, E. Cordoncillo, Pigments based on Cr and Sb doped TiO<sub>2</sub> prepared by microemulsion-mediated solvothermal synthesis for inkjet printing on ceramics, *Dyes and Pigments*, 116 (2015) 106-113.
- [8] R.Z. Ma, J. Wu, B.Q. Wei, J. Liang, D.H. Wu, Processing and properties of carbon nanotubes–nano-SiC ceramic, *J. Mater. Sci.*, 33 (21)(1998) 5243-5246.
- [9] O. Ola, M.M. Maroto-Valer, Review of material design and reactor engineering on TiO<sub>2</sub> photocatalysis for CO<sub>2</sub> reduction, *J. Photoch. Photobio. C*, 24 (2015) 16-42.
- [10] Y.Q. Wu, Y.F. Zhang, X.X. Huang, J.K. Guo, Preparation of platelike nano alpha alumina particles, *Ceram. Inter.*, 27 (3)(2001) 265-268.
- [11] A. Nakahira, K. Niihara, Sintering behaviors and consolidation process for Al<sub>2</sub>O<sub>3</sub>/SiC nanocomposites, *J. Ceram. Soc. JPN*, 100 (1160)(1992) 448-453.
- [12] J. Li, H. Liao, L. Hermansson, Sintering of partially-stabilized zirconia and partially-stabilized zirconia—hydroxyapatite composites by hot isostatic pressing and pressureless sintering, *Biomaterials*, 17 (18)(1996),1787-1790.

- [13] J.D. Katz, Microwave sintering of ceramics, *Annu. Rev. Mater. Sci.*, 22 (1)(1992) 153-170.
- [14] T.T.T. Hien, T. Shirai, M. Fuji, An advanced fabrication route for alkali silicate glass by non-firing process. *Adv. Powder Technol.* 25(1) (2014) 360-364.
- [15] E.U. Apiluck, T. Shirai, K. Tomoaki, K. Orito, H. Watanabe, M. Fuji, M. Takahashi, Novel fabrication route for porous ceramics using waste materials by non-firing process, *J. Ceram. Soc. Jpn.* 118 (1380)(2010) 745-748.
- [16] G. Gorrasi, A. Sorrentino, Mechanical milling as a technology to produce structural and functional bio-nanocomposites, *Green Chem.* 17(5)(2015) 2610-2625.
- [17] T. Shirai, K. Orito, T.T.T. Hien, M. Fuji, Effects of different forming methods on the properties of solidified body by non-firing process through the mechanochemical treatment, *J. Jpn. Soc. Powder. Powder. Met.* 59 (9)(2012) 517-521.
- [18] M. Yang, C. Xu, C. Wu, K.C. Lin, Y.J. Chao, L. An, Fabrication of AA6061/Al<sub>2</sub>O<sub>3</sub> nano ceramic particle reinforced composite coating by using friction stir processing, *J. Mater. Sci.*, 45 (16)(2010) 4431-4438.
- [19] O. Ikkala, G. Brinke, Functional materials based on self-assembly of polymeric supramolecules, *Science*, 295 (5564)(2002) 2407-2409.
- [20] J.A. Van Vliet, J.J. Geijtenbeek, U.S. Patent No. 5,973,453, Washington, DC: U.S. Patent and Trademark Office. (1999)
- [21] H. Kishi, Y. Mizuno, H. Chazono, Base-metal electrode-multilayer ceramic capacitors: past, present and future perspectives, *JPN J. Appl. Phys.*, 42 (1)(2003) 1.

- [22] E.A. Nenasheva, A.D.Kanareykin, N.F.Kartenko, A.I. Dedyk, S.F. Karmanenko, Ceramics materials based on (Ba, Sr) TiO<sub>3</sub> solid solutions for tunable microwave devices, *J. Electroceram.*, 13 (1-3)(2004) 235-238.
- [23] E. Traversa, Ceramic sensors for humidity detection: the state-of-the-art and future developments, *Sensor. Actuat. B: Chem.*, 23 (2-3)(1995) 135-156.
- [24] S. Zhou, Z. Wang, X. Sun, J. Han, Microstructure, mechanical properties and thermal shock resistance of zirconium di-boride containing silicon carbide ceramic toughened by carbon black, *Mater. Chem. Phys.*, 122 (2-3)(2010) 470-473.
- [25] M.E. Achour, M. E. Malhi, J.L. Miane, F. Carmona, F. Lahjomri, Microwave properties of carbon black-epoxy resin composites and their simulation by means of mixture laws, *J. appl. Polym. Sci.*, 73 (6)(1999) 969-973.
- [26] S. Iijima, Helical microtubules of graphitic carbon, *nature*, 354 (6348)(1991) 56.
- [27] P.G. Collins, P. Avouris, Nanotubes for electronics, *Sci. am.*, 283 (6)(2000), 62-69.
- [28] M.J. Treacy, T.W. J.M. Ebbesen, Gibson, Exceptionally high Young's modulus observed for individual carbon nanotubes, *Nature*, 381 (6584)(1996) 678.
- [29] M.R. Falvo, G.J. Clary, R.M. Taylor, V. Chi, F.P. Brooks Jr, S. Washburn, R. Superfine, Bending and buckling of carbon nanotubes under large strain, *Nature*, 389 (6651)(1997) 582.
- [30] A. Peigney, C. Laurent, A. Rousset, Synthesis and characterization of alumina matrix nanocomposites containing carbon nanotubes, In *Key Engineering Materials* (Vol. 132, pp. 743-746) (1997), Trans Tech Publications.

- [31] R. Kamalakaran, F. Lupo, N. Grobert, D. Lozano-Castello, N.Y. Jin-Phillipp, M. Rühle, In-situ formation of carbon nanotubes in an alumina–nanotube composite by spray pyrolysis, *Carbon*, 41 (14)(2003) 2737-2741.
- [32] S. Rul, C. Laurent, A. Peigney, A. Rousset, Carbon nanotubes prepared in situ in a cellular ceramic by the gel casting-foam method. *J. Euro. Ceram. Soc.*, 23 (8)(2003) 1233-1241.
- [33] S. Rul, F. Lefèvre-Schlick, E. Capria, C. Laurent, A. Peigney, Percolation of single-walled carbon nanotubes in ceramic matrix nanocomposites *Acta Mater.*, 52 (4)(2004) 1061-1067.
- [34] J. Hilding, E.A. Grulke, Z. George, F. Lockwood, Dispersion of carbon nanotubes in liquids, *J. disper. sci. technol.*, 24 (1)(2003) 1-41.
- [35] K.L. Lu, R.M. Lago, Y.K. Chen, M.L.H. Green, P.J.F. Harris, S.C. Tsang, Mechanical damage of carbon nanotubes by ultrasound, *Carbon*, 34 (6)(1996) 814-816.
- [36] Y. Wang, J. Wu, F. Wei, A treatment method to give separated multi-walled carbon nanotubes with high purity, high crystallization and a large aspect ratio, *Carbon*, 41 (15)(2003) 2939-2948.
- [37] Y.B. Li, B.Q. Wei, J. Liang, Q. Yu, D.H. Wu, Transformation of carbon nanotubes to nanoparticles by ball milling process, *Carbon*, 37 (3)(1999) 493-497.
- [38] Z. Jia, Z. Wang, J. Liang, B. Wei, D. Wu, Production of short multi-walled carbon nanotubes, *Carbon*, 37 (6)(1999) 903-906.
- [39] M.S. Shaffer, X. Fan, A.H. Windle, Dispersion and packing of carbon nanotubes, *Carbon*, 36 (11)(1998) 1603-1612.

- [40] J. Sun, L. Gao, Development of a dispersion process for carbon nanotubes in ceramic matrix by heterocoagulation, *Carbon*, 41 (5)(2003) 1063-1068.
- [41] J. Liang, L. Gao, Modified carbon nanotubes: an effective way to selective attachment of gold nanoparticles, *Carbon*, 41 (15)(2003) 2923-2929.
- [42] L. Zhao, L. Gao, Stability of multi-walled carbon nanotubes dispersion with copolymer in ethanol, *Colloid. Surface. A: Physicochemical and Engineering Aspects*, 224 (1-3)(2003) 127-134.
- [43] J. Ning, J. Zhang, Y. Pan, J. Guo, Surfactants assisted processing of carbon nanotube-reinforced SiO<sub>2</sub> matrix composites, *Ceram. Int.*, 30 (1)(2004) 63-67.
- [44] F. Zhang, J. Shen, J. Sun, Processing and properties of carbon nanotubes-nano-WC-Co composites, *Mater. Sci. Eng.: A*, 381 (1-2)(2004) 86-91.
- [45] M.Q. Ye, L.L. He, A.J. Han, Conductivity mechanism and electrical properties influence factors of filling conductive polymer composite materials. *New Chemical Materials*, 36 (11)(2008) 13-15.
- [46] K. Miyasaka, K. Watanabe, E. Jojime, Electrical conductivity of carbon-polymer composites as a function of carbon content, *J. Mater. Sci.*, 17 (6)(1982) 1610-1616.
- [47] K. Miyasaka, K. Watanabe, E. Jojime, Electrical conductivity of carbon-polymer composites as a function of carbon content, *J. Mater. Sci.*, 17 (6)(1982) 1610-1616.
- [48] L.K.H. Vanbeek, B.I.C.F. Vanpul, Internal field emission in carbon black-loaded natural rubber vulcanizes, *J. Appl. Polym. Sci.*, 6 (24)(1962) 651-655.

- [49] J.C. Huang Carbon black filled conducting polymers and polymer blends, *Adv. Polym. Technol.*, 21 (4)(2002) 299-313.
- [50] C. Zhang, C.A. Ma, P. Wang, Temperature dependence of electrical resistivity for carbon black filled ultra-high molecular weight polyethylene composites prepared by hot compaction, *Carbon*, 43 (12)(2005) 2544-2553.
- [51] B. Adohi, J.P. Mdarhri, A. Prunier, A comparison between physical properties of carbon black-polymer and carbon nanotubes polymer composites, *J. Appl. Phys.*, 108 (7)(2010) 074108-11.
- [52] J.H. Du, J. Bai, H.M. Cheng, The present status and key problems of carbon nanotube based polymer composites, *Exp. Polym. Lett.*, 1 (5)(2007) 253-273.



## **Chapter2 Micro-phase Separation Process to Prepare Carbon Nanoparticles Added Functional Polymer Membrane with Network Structure**

### **2.1 Introduction**

Due to the viable application in conductive materials and electromagnetic shielding areas, functional nanoparticle networks with isotropic arrays, hydrophobicity and conductivity have attracted much attention. This array of particles was usually manufactured by photolithography and printed directly on the substrate, with woven polymer fibers of electrically conductive particles [1]. However, these processes were extensive, require precise nanotechnology, and it is difficult to obtain the desired network structure.

Micro-phase separation technology was the most common method for preparing and producing polymer films [2]. As a phase separation technology, the dry casting process generally required a ternary reaction system, including a macromolecular substance, a good-solvent with a low boiling point, and a non-solvent with a high boiling point [3]. When the ternary solution was poured onto the substrate, the solvent begins to evaporate first. The solute polymer gas then separated from its non-solvent due to the reduced solubility in the solution. After vaporization to remove the non-solvent, the 3D polymer network appeared as membrane morphology. For ternary system components, hydrophobic cellulose acetates were most often chosen for film formation by the micro-phase separation process [5] because of their rust, chemical stability and environmental friendliness. Casting polymer solutions of CA, acetone and water were studied due to thermodynamic possibility and tunability [2,6,7].

It was currently being evaluated to modify the insulating polymer by adding

certain fillers such as minerals [8], metal powders [9,10], graphite fibers [11] and carbon black (CB) [12] because the polymer properties improved on the polymerization toughness, strength and functional applications such as thermal conduction [13] and electrical conduction [14]. Considering the conductivity and affinity with cellulose acetate, the electrical conductivity of carbon was much smaller than that of metal powder, and the oxidation resistance when formed with a polymer had a distinct advantage over metal. At the same time, Van Der Waals's high surface area carbon particle strength ensured that the attraction of adjacent particles was almost stick together, and a reasonable amount [15] was used for thermo conduction and electro conduction.

Carbon nanoparticles were used as fillers in cellulose acetate in this study. Network membranes were prepared by micro-phase separation process to improve polymer conductivity. The nanocarbon nanoparticles were added to the ternary system and micro-phase separated to form a CA polymer network. The non-solvation initiated the thermodynamic compatibility of the carbon nano particles and the ternary solution. In summer, the surface properties of the nanoparticles affected the binding force of the particles. Therefore, the CA polymer network with carbon nanoparticles added could be easily prepared. After removal of the polymer composition by heating, the functional properties of conductivity were measured. The ternary system, the ratio of carbon nanoparticles and the heat treatment temperature were studied to optimize the morphology of the network membrane.

## **2.2 Experimental Section**

### **2.2.1 Materials**

This experiment used a cellulose acetate with a molecular weight of 50,000 g/ml

(CA, Aldrich Chemical Company Inc., acetyl content: 39.8 wt%, Mn: 30,000) as a polymer coated on a quartz substrate (1.5 \* 25 \* 70 mm). The dry film was prepared by dry-casting. Acetone (Wako Pure Chemical Industries, Ltd., analytical grade, bp: 56.5°C) was used as a good-solvent and distilled water as a non-solvent. Thereafter, the ratio of the weight percentages of the polymer and the non-solvent in the ternary solution was abbreviated as P and N. Hydrophobic carbon nanoparticles (diameter 70 nm, Lion Corporation) were filled into the ternary system solution to prepare a polymer film.

#### 2.2.2 Preparation of ternary system membrane and carbon nanoparticle added membrane

The ternary solution was cast onto a quartz support and a porous membrane was prepared due to the evaporation of acetone. In the case of 20% humanity, the cast film was kept under stable conditions at room temperature to evaporate non-solvent and residual good solvent. The casting thickness 12  $\mu\text{m}$  was controlled with an automatic bar coater (K Control Coater, RK Print Coat Instruments Ltd.) at a speed of 3 cm/s.

Considering the good affinity between the poor solubility of the particles/good solvent and the particle/non-solvent, hydrophobic carbon nanoparticles (diameter 70 nm) were added to the ternary system to prepare different concentrations (2.7, 4, 8 wt.%) and P3N15 solution components (for example, P3N15 indicates the ratio of polymer to non-solvent were 3% and 15%, respectively). The preparation process is actually the same as the initial film. The prepared film was heated and maintained at 300°C., 350°C. and 400°C. in an argon atmosphere for 2 hours to remove cellulose acetate to obtain a network of particles on the substrate.

### 2.2.3 Characterizations

The surface morphology of the dry membrane was examined with a optical microscope (OLS4000, Olympus Corp.), and a scanning electron microscope (SEM, JSM-7000F, JEOL Ltd.) observations were performed and samples were coated with helium (Osmium plasma coater OPC60A, Filgen). The conductivity of the network membrane was measured by the Four-probe Van Der Pauw method [16] after the heat treatment process.

## 2.3 Results and Discussion

Minor changes in the dry casting process can significantly affect the membrane morphology and are quite sensitive to the preparation conditions. Note that the compositional ratio dependence of the ternary solution is the main experimental aspect of the film's characteristic structure. In addition, previous studies have focused mainly on cross-sectional views of relatively thick polymer films because they contain macro voids or finger-like passageways [2], so that the thickness of the prepared polymer film is several hundred micrometers. In order to study the influence of the composition of the casting solution on the overall thickness, a 12  $\mu\text{m}$  thick wet film was produced in this work.

### 2.3.1 Membrane of CA/Ace/W ternary system

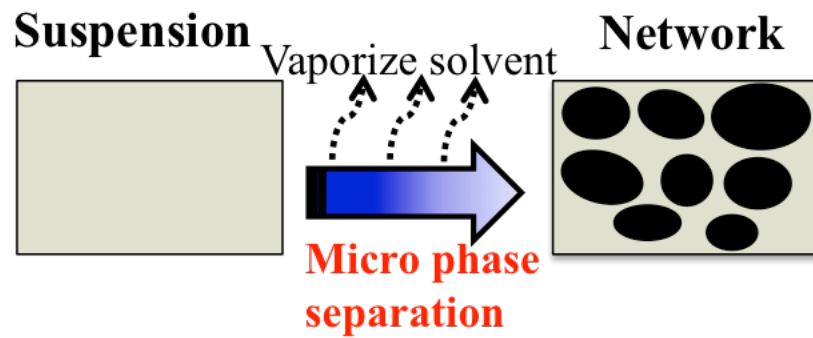


Fig. 2.1. Illustration of process during non-solvent inducing micro phase separation.

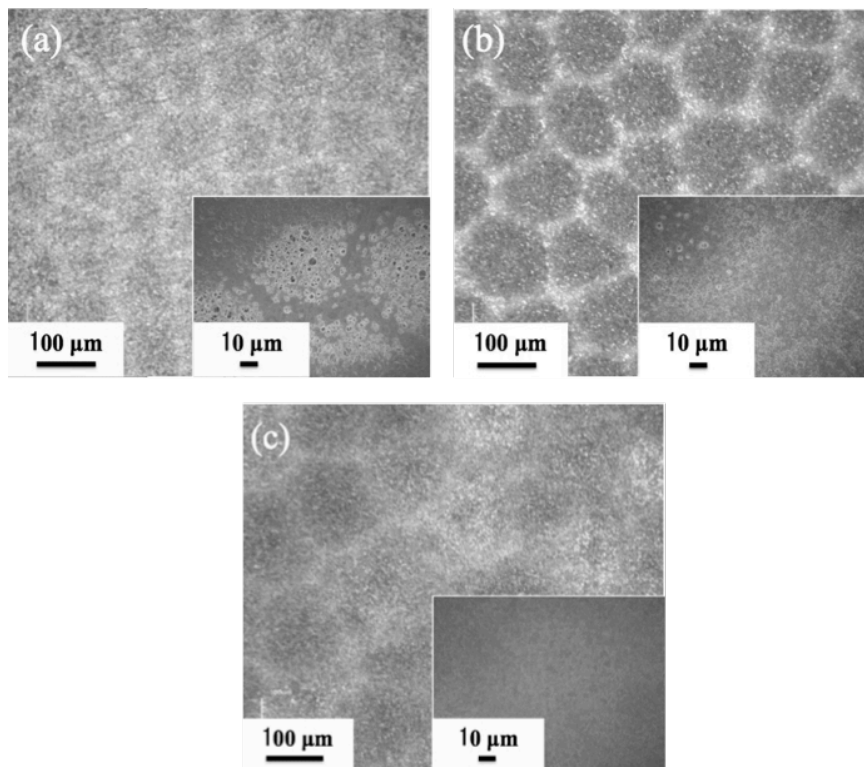


Fig. 2.2. Optical microscope and SEM images of polymer membrane corresponding to CA/water ratios of P3N15, P4N14 and P5N13.

Fig. 2.1 illustrates the micro phase separation process of cellulose acetate/acetone/water ternary system and Fig. 2.2 shows the upper-face morphology of

membranes via micro-phase separation. The final membrane structures impacted by compositions of initial ternary solution were changed by means of the concentration controlling, which kept the good-solvent fixed at 80 wt.% and the weight fraction of polymer and non-solvent were P3N15, P4N14 and P5N13, respectively.

The SEM images revealed ordered polygonal (pentagons and hexagons) unit network and asymmetric pores surrounded by polygon from top-view. We believe that these self-assembly modes were due to the Marangoni effect, which as caused by the rapid evaporation process. The volatile solution film deposited on the substrate was applied to a rapid temperature change between the substrate and the free upper surface, conducted enough heat and create a temperature gradient in the movie. It means that the formation of polygons is driven by Marangoni instability [3].

Focusing on the center of the polygon, it can be clearly seen from these images that an asymmetric 3D porous network membrane is formed by the micro-phase separation process. Figure 2.2 shows that as the P/N ratio in the initial casting solution increases, the membrane structure changes from high porosity to virtually no porosity. As can be seen from Figure 2.2(a), the isotope film prepared from the 3/15 P/N ratio is highly porous. During film formation, polymer and non-solvent concentration gradients are formed along the film thickness. Figure 2.2(b) shows a P4N14 film with a blurred edge between individual polygons. An increase in the percentage of polymer leads to a smaller pore size trend than a high percentage. At the highest percentage of polymer, the pore size and distribution become uniform from Figure 2.2(c) and the pore units cannot be determined. The wet thickness of the coating was 12  $\mu\text{m}$ , and the average dry thickness value obtained by the optical microscope was 5  $\mu\text{m}$ .

### 2.3.2 Membrane of carbon nanoparticles added CA/Ace/W ternary system

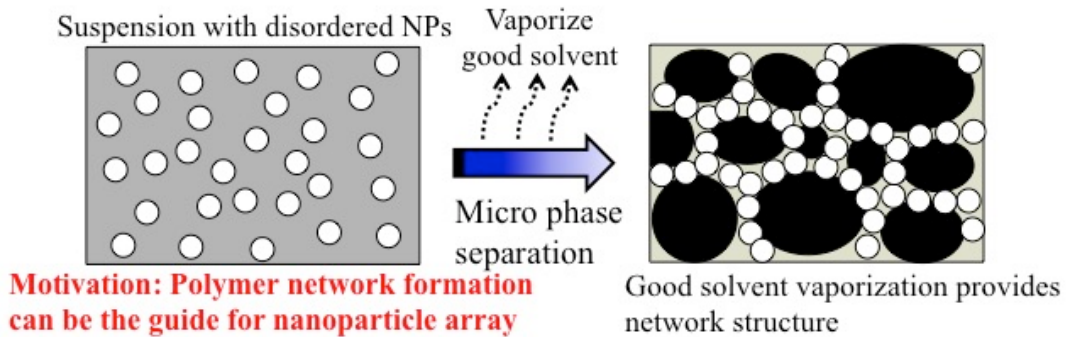


Fig. 2.3. Illustrate of the micro phase separation process of cellulose acetate/acetone/water ternary system.

Fig. 2.3 illustrates the micro-phase separation process of cellulose acetate/acetone/water ternary system with carbon nanoparticles added. As the most suitable ratio with asymmetric network morphology, P3N15 is designed for further discussion. From the SEM image of Figure 2.4 it can be seen that carbon particles are located in the polymer network due to the low solubility of hydrophobic particles in water and the strong interfacial chemical interactions between the particles/polymer materials.

Reduction of carbon particle concentration from 8 to 2.7% by weight facilitates the formation of continuous membrane morphology with less porosity in the network. The structure containing the quantitative polymer portion depends on the quantification of the particles. Figure 2.4(a) shows the porosity of the membrane as predicted by this model. The mesh diameter 2.4 (c) is 2.7% by weight of the particle content. Based on these results, we can confirm that nanoparticles, including network membranes, can be simply prepared by a micro-phase separation process.

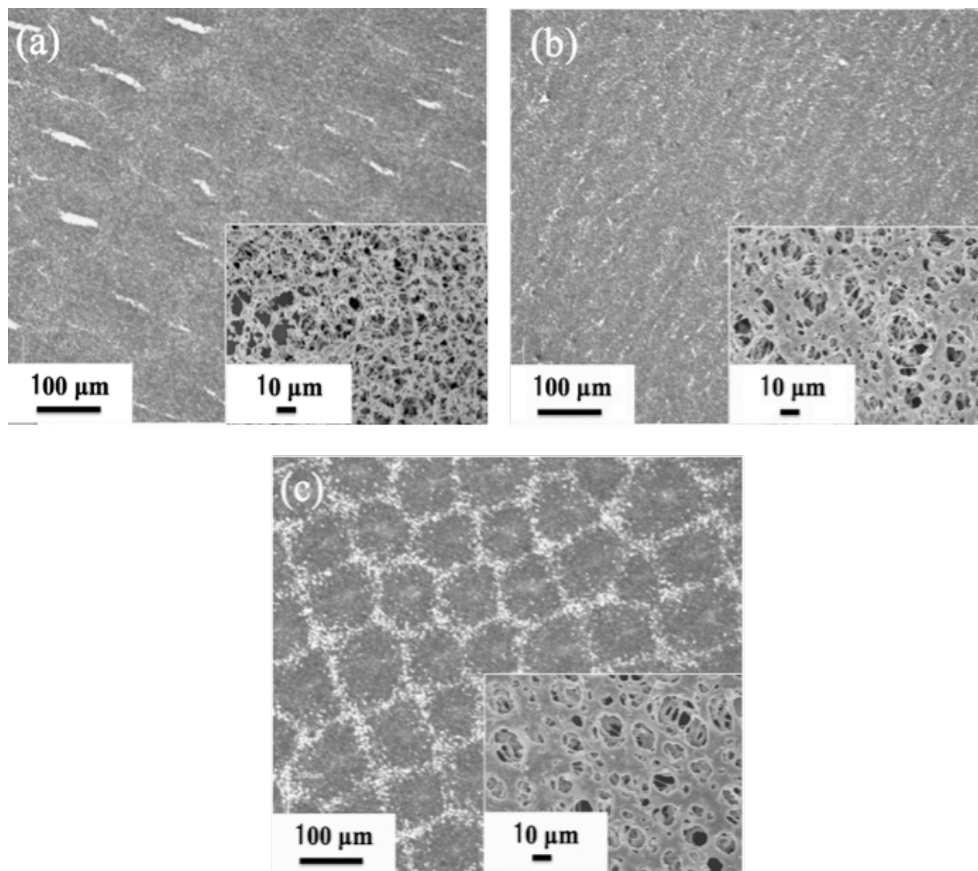


Fig. 2.4. P3N15 optical microscope and scanning electron micrographs of membrane from carbon nanoparticle added CA/acetone/water solution corresponding to particle weight percent.

Assume that higher amounts of particles require more polymer to surround them. In addition, carbon particles tend to agglomerate when a large amount of polymer is added to the system. The increase in cracks and fractures of the polymer film is due to a decrease in the tensile yield strength when carbon agglomeration occurs. Considering the above situation, the high particle concentration in Fig. 2.5(a) apparently overflows to a larger gap in the unit polygon. The entrapped polymer network structure in Figure 2.5(b) illustrates that the lower ratio of particles to polymer material favors particle

connectivity and film continuity. The microporous in separation process proposes the most asymmetric structure and the optimal compositional ratio that are most favorable for the preparation of nanoparticles containing a uniform polymer network (Figure 2.5(c)).

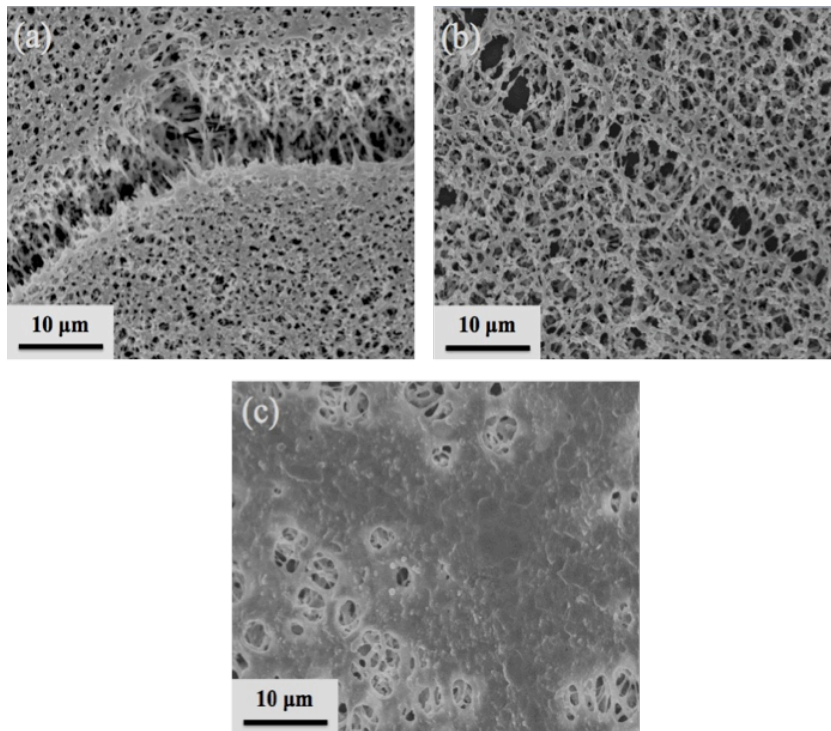


Fig. 2.5. P3N15 SEM images of different weight percent (a) 8%, (b) 4% and (c) 2.7% at polygon edge in membrane from carbon nanoparticle added water included ternary system corresponding to particle.

### 2.3.3 Heat treatment and electro-conductivity of membrane

Insulating polymers are generally considered to be dispersed in different materials for functional applications such as traffic subsections, electronics industry and equipment industry applications [5]. Fillers such as carbon nanoparticles enhance the conductivity of the polymer [4]. In order to reinforce the physical process that electrical

TG/DTA has been used to measure weight changes and technical depreciation conditions involving the electrical conductivity of the network membrane, the heat treatment with an oxygen-free atmosphere can be collapsed in the face without removing the polymer and the original particle network structure. The TG/DTA curve for pure cellulose acetate is shown in Figure 2.6. From the curves, decomposition and depolymerization occurred at 325°C-380°C, and the CA polymer weight loss was 83%.

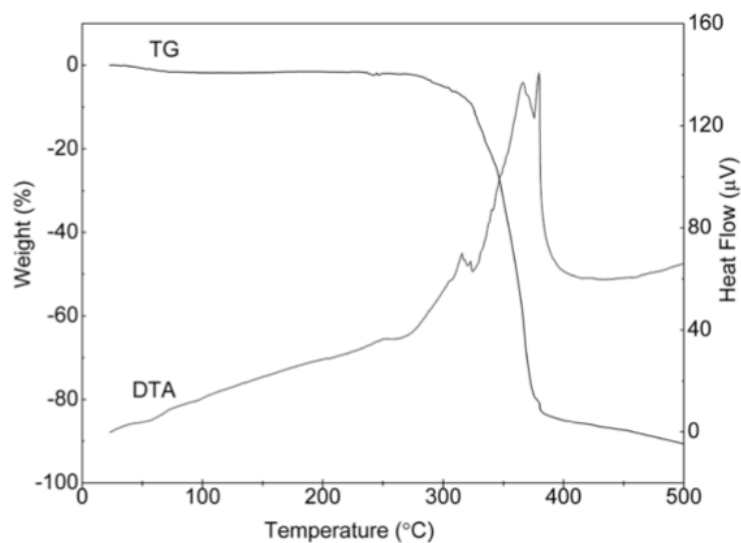


Fig. 2.6. TG-DTA curve of cellulose acetate.

The morphology of the film treated by heat is shown in Figure 2.7, in which the decomposition of the particles containing CA results in the formation of a pure particle asymmetric network. In addition, due to the nanoparticle effect, even if the polymer once used as a binder has been removed, the remaining carbon particles are still connected to each other to maintain the network structure.

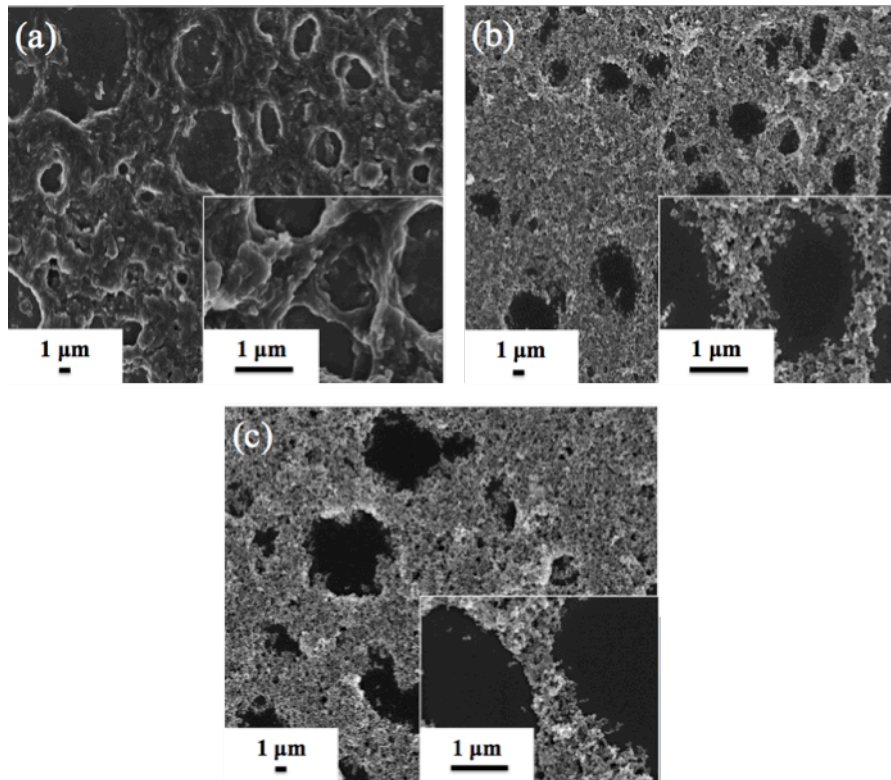


Fig. 2.7. Scanning electron micrographs of P3N15 solution ratio with 4wt.% carbon nanoparticle added membrane heated under (a)300 °C, (b)350 °C and (c)400 °C, respectively.

## 2.4 Conclusion

To obtain carbon nanoparticle network structure, membrane was simply prepared by micro-phase separation of cellulose acetate/acetone/water system under heating at 300°C/350°C/400°C. As a particle network structure, the ordered arrangement of conductive pathways significantly improves the electrical conductivity of carbon nanoparticles. Further research based on various particles can be provided to enable the application based on nanoparticle properties and network structure.

## References

- [1] C. Takai, A. Tamura, M. Fuji, Synthesis of Silver Nanoparticle Network

- Induced by a Micro-phase Separation, *Advanced Powder Technology*, 25 (2014) 621 - 624.
- [2] S.A. Altinkaya, H. Yenil, B. Ozbas, Membrane Formation by Dry-cast Process Model Validation Through Morphological Studies, *J. Membr Sci.*, 249 (2005) 163 - 172.
- [3] G. Philipp, H. Schmidt, *J. Non-Crystal. Solid*, 63 (1984) 283 - 293.
- [4] S.S. Shojaie, W.B. Krantz, A.R. Greenberg, Dense Polymer Film and Membrane Formation via the Dry-cast Process; Part 1. Model Validation and Morphological Studies, *J. Membr Sci.*, 94 (1994) 281 - 298.
- [5] G.R. Guillen, Y. Pan, M. Li, E.M.V. Hoek, Preparation And Characterization of Membrane Formed by Nonsolvent Induced Phase Separation: A Review, *Ind. Eng. Chem. Res.*, 50 (2011) 3798 - 3817.
- [6] A.J. Reuvers, C.A. Smolders, Formation of Membrane by Means of Immersion Precipitation, Part II. The Mechanism of Formation of Membranes Prepared From the System Cellulose Acetate-Acetone-Water, *J. Membr Sci.*, 34 (1987) 67 - 86.
- [7] N. Vogrin, Č. Stropnik, V. Musil, M. Brumen, The Wet Phase Separation: the Effect of Cast Solution Thickness in the Appearance of Macrovoids in the Membrane Forming Ternary Cellulose acetate/acetone/water System, *J. Membr Sci.*, 207 (2002) 139 - 141.
- [8] E.G. Viakh, E.F. Panarin, T.B. Tennikova, K. S, C. K, Development of Multifunctional Polymer mineral Composite Materials for Bone Tissue Engineering, *J. Biomed. Mater. Res.*, 75A (2005) 333 - 341.
- [9] J.J. Watkins, T.L. McCarthy, Polymer/Metal Nanocomposite Synthesis in

- Supercritical CO<sub>2</sub>, Chem. Mater., 7 (1995) 1991 - 1994.
- [10] L, Yang, D.L. Schruben, Electrical resistivity behavior of mold-cast metal-filled polymer composites, Polym. Eng. Sci., 34 (1994) 1109 - 1114.
- [11] V. Haddadi-Asi, M. Kazacos, M. Skyllas-Kazacos; Carbon-polymer composite electrodes for redox cells. J. Appl. Polym. Sci.; 57 (1995) 1455 - 1463.
- [12] J.C. Huang, Carbon Black Filled Conducting Polymers and Polymer Blends, Adv. Polym. Tech., 21 (2002) 299 - 313.
- [13] G.W. Lee, M. Park, J. Kim, JI. Lee, HG. Yoon, Enhanced thermal conductivity of polymer composites filled with hybrid filler, Composites Part A, 37 (2006) 727 - 734.
- [14] D.M. Bigg, D.E. Stutz, Plastic Composites for Electromagnetic Interference Shielding Applications, Polym. Compos. 4 (1983) 40 - 46.
- [15] R. Schueler, J. Petemann, K. Schulte, H. Wentzel, Agglomeration and Electrical Percolation Behavior of Carbon Black Dispersed in Epoxy Resin, J. Appl. Polym. Sci., 63 (1997) 1741 - 1746.
- [16] M. Wakeshima, H. Masuda, K. Yamada, N. Sato, T. Fujino, New Measurement System of Specific Resistivity and Hall Coefficient by Four-probe Van Der Pauw Method, Tohoku University.



## **Chapter 3 Preparation and Discussion on Carbon Nanoparticles/Silica Composite Ceramics Fabricated by Non-Firing Ceramic Process**

### **3.1 Introduction**

This chapter aimed to prepare carbon nanoparticles/silica non-fired 3D ceramic matrix by calcination solidification method and discusses the mechanical and electrical properties of sample. The chemical reaction in forming this solidified body was due to dehydration/condensation reaction of silicate ions eluted from silica particles [1-3]. However, when a hydroxyl group was present on the surface of carbon particles, this reaction system would react with the functional group [4]. Also, the presence or absence of reaction with carbon atoms in carbon particles was not known. Therefore, in this chapter, the microstructure of carbon nanoparticles/silica non-fired solidified ceramic body was evaluated to discuss the presence or absence of bonding between silica particles and carbon particles, and also the relationship between them and physical properties were also investigated.

### **3.2 Experimental section**

#### **3.2.1 Materials and preparation**

In this experiment, amorphous silica (SO-C1 prepared by VMC method, Admatechs Company Limited) and carbon nanoparticles (AGB - 20, ITO Graphite Industry Co., Ltd.) were used as raw material powders. In addition, 1 M of KOH aq. was used as a reaction solution.

Surface activation treatment was performed on amorphous silica under the conditions of Table 3.1 using a planetary ball mill (Pulverisette 5, Fritsch). The treated silica and graphite were weighed under the conditions of 10, 20, 30, 40, 50, 60, 70, 80,

and 90 vol. % and mixed for 17 hours using a pot mill under the conditions in Table 2-3. Then 1 M KOH aq. was added and mixed, and it was defoamed using a rotation / revolution mixer (ARV-930TWIN, THINKY) (Table.3.1). After curing for 5 hours in a dryer at 80°C., the mold was demoded and further dried at room temperature for 17 hours to evaluate.

Table 3.1 The surface-activated condition by planetary ball mill.

Rotation speed	200 rpm
Milling time	15 min
Milling pod	YSZ, 500ml
Ball weight	400 g
Milling ball	YSZ, 5 mm
Powder weight	100 g

Table 3.2 Experimental conditions.

Milling pod	PP, 100 ml
Milling ball	Zirconia balls
Milling time	17 h
Powder weight	silica (SO-C1): 15 g

### 3.2.2 Characterization

A transmission electron microscope (TEM) (JEM-2100F, JEOL Limited) observes the morphology of a ceramic body by a scanning electron microscope (SEM) (JSM-7000F, JEOL Limited). For the characteristics, electric conductivity was measured by the 4-probe Van der Pauw method [5]. Bending strength of the ceramic

bulk was measured using a precision universal/tensile tester (AGS-G series, Shimadzu Corporation) having an average of 5 samples. The measurement progressed at 0.5% mm/min crosshead speed at room temperature and the dimensions of the sample were fixed to 0.5 cm × 1 cm × 5 cm (thickness × width × length).

### **3.3 Illustration for measurement of electrical conductivity**

DC four-terminal Van der Pauw method was used for the evaluation of electrical conductivity. There are two roughly divided: two-probe method and four-probe method to measure electrical property. The two-probe method measures the sample with two electrodes, and this method has the merit that measurement is simple, but there is a disadvantage that it is influenced by the contact resistance at the electrode because current supply and voltage measurement are performed on the same electrode. Therefore, in this experiment measurement was taken using the four-probe method. Although contact resistance does not affect, there is a disadvantage that it has some trouble in sample preparation.

The measurement sample was prepared in the following procedure. Cut the prepared samples into a size of  $\Phi 16 \times 1.5$  mm using a diamond cutter and attach a silver paste on the diagonal line to the sample. For the measurement, a DC voltage / current source / monitor (R6243, manufactured by Advantest Corporation) was used. The applied current was set at 0.5  $\mu$ A to 500 mA and the change in voltage was recorded. The calculation formula of DC four-probe Van der Pauw method is shown in equation (3-1) [5]. The condition for establishing the approximation of the expression (3) for obtaining the parameter  $f$  is the case where  $R_{AB, CD} - R_{BC, DA}$  is small. That is, this formula cannot be used when the difference in resistance value depending on the direction of the measurement sample is large. The electric resistivity was converted to

the electric conductivity using the formula (3-3).

$$\rho = \frac{\pi d}{\ln 2} \cdot \frac{R_{AB,CD} + R_{BC,DA}}{2} \cdot f \cdot \left( \frac{R_{AB,CD}}{R_{BC,DA}} \right) \quad (3-1)$$

$$f \approx 1 - \left( \frac{R_{AB,CD} - R_{BC,DA}}{R_{AB,CD} + R_{BC,DA}} \right)^2 \cdot \frac{\ln 2}{2} - \left( \frac{R_{AB,CD} - R_{BC,DA}}{R_{AB,CD} + R_{BC,DA}} \right)^4 \left[ \frac{(\ln 2)^2}{4} - \frac{(\ln 2)^3}{12} \right] \quad (3-2)$$

$$\rho = \frac{1}{\sigma} \quad (3-3)$$

$\rho$ : Electric resistivity [ $\Omega \cdot \text{m}$ ]

$R$ : Resistance value [ $\Omega$ ]

$d$ : Sample thickness [m]

$\sigma$ : Electric conductivity [S/m]

### 3.4 Results and discussion

#### 3.4.1 Morphology of carbon nanoparticle/silica ceramic composites

Figure 3.1 shows typical SEM images of a cross-sectional view of carbon nanoparticle/silica ceramic composites. By increasing the amount of CNTs from 10% to 90%, it can be clearly observed from the figures that the carbon nanoparticle homogenously dispersed and mixed with silica without affecting the formation and curing of the ceramic matrix. Meanwhile, after the non-fired preparation process, no structure other than carbon material and nanotubes can function at lower temperatures compared to other copper processes. Also, silica combined to form a ceramic matrix for ensuring the mechanical strength.

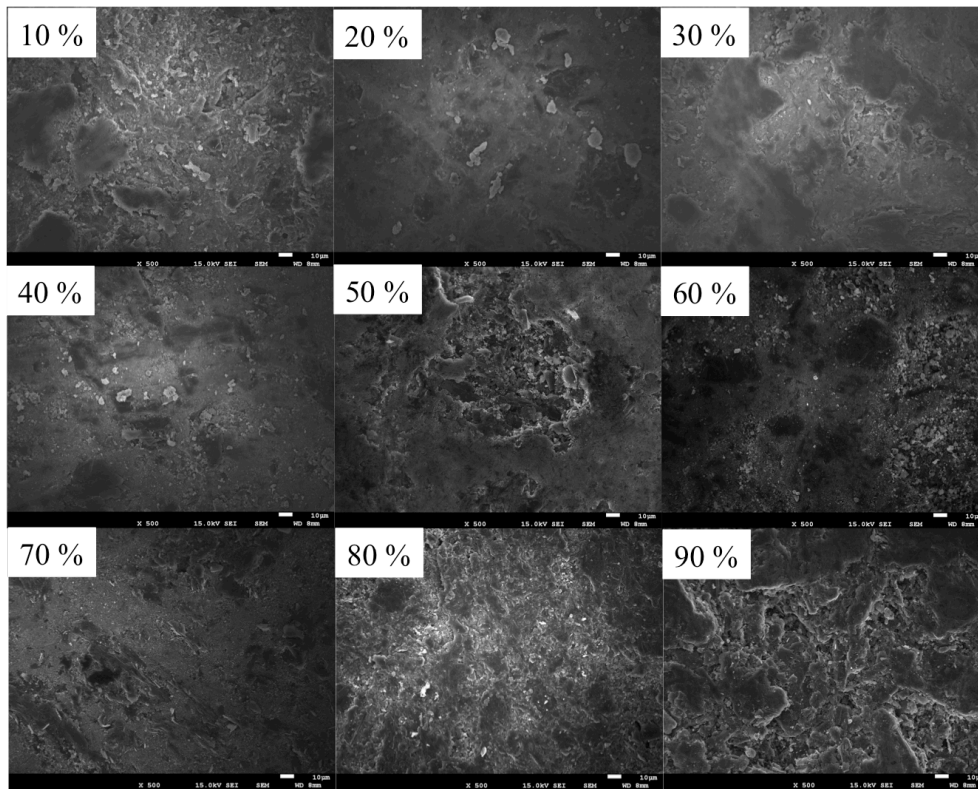


Fig.3.1. SEM images of composites with different carbon nanoparticles volume percentage from 10% to 90%.

### 3.4.2 Electro-conductivity and bending strength

Table. 3.3 Mechanical and electrical properties of carbon nanoparticles/silica composites.

Carbon amount vol.%	Bending strength Mpa	Electrical resistivity $\Omega \text{ cm}^{-1}$
10	9.815	5.6E+01
20	15.225	5.7E+01
30	14.058	6.1E+01
40	9.775	1.6E-03
50	8.826	2.8E-04
60	8.538	9.8E-05
70	4.303	4.4E-05
80	4.003	1.5E-05
90	-	3.9E-06

The results of the electric conductivity and the result of the strength test in the carbon nanoparticles mixed concentration change are summarized in both table. 3.3 and fig. 3.2. Conductivity varies greatly between carbon nanoparticles volume percentage of 30% and 40%. When the content ratio of carbon nanoparticles is 30% or less than it, the electrical resistivity becomes around  $60 \Omega \text{ cm}^{-1}$ , and when the carbon nanoparticles content is 40 vol.% or higher than it, an decrease in electrical resistivity can be observed. It is considered that there is a rate at which carbon nanoparticles percolate between 60% and 70%. Resistivity is much more lower when silica 70% or more. This will be considered together with the results of the following structural analysis. The electrical

resistivity decreases steadily at a ratio of the silica ratio of 60% or more. The reason for this seems to be attributable to an increase in the amount of conductive paths accompanying an increase in the number of conductive particles. Also, if silica particles are present between carbon nanoparticles particles, even if the carbon nanoparticles are close to each other, resistance develops, but as resistance decreases as carbon nanoparticles increases, conductivity may continue to decrease.

Fig. 3.2 also shows the result of calculating the bending stress at each ratio from the result of three-point bending test. A solidified body was prepared for carbon nanoparticles 10% to 90%, But measurement could not be performed because all samples collapsed while processing for measurement. When the carbon nanoparticles content is 20% and higher, the strength decreased with increasing carbon nanoparticles. When the carbon nanoparticles ratio is between 30% and 40%, The bending strength greatly decreases. This concentration is in agreement with the value where the electric conductivity greatly changed, which seems to be due to the percolation of the carbon nanoparticles filler. The reason for showing the strength from the reaction mechanism

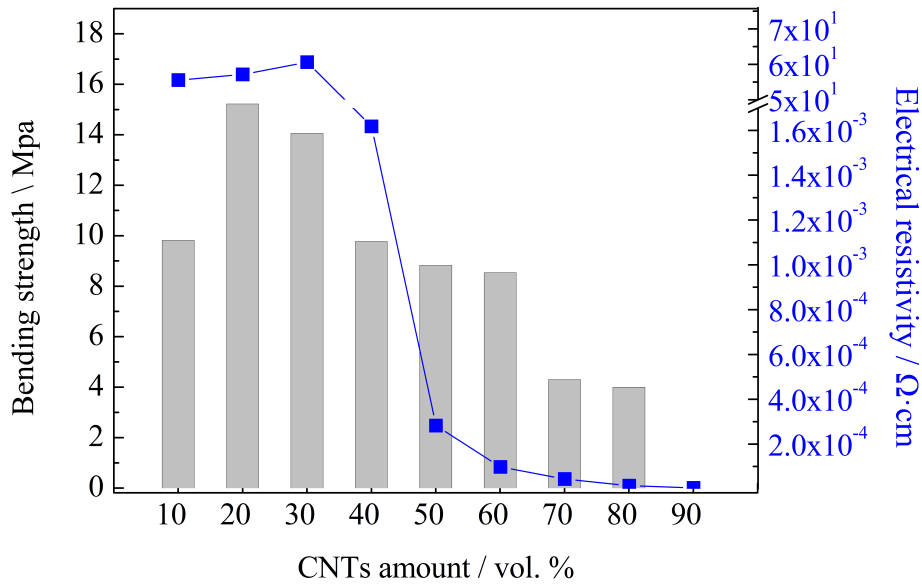


Fig. 3.2. The mechanical properties and mechanical properties of carbon nanoparticle/silica using non-firing process

of this experiment is binding due to re-elution between the silica particles. That is, if silica is bonded to the whole, the strength is considered to be high. When carbon nanoparticles is 40% or higher than it, carbon nanoparticles is percolated, whereas silica does not bond throughout the system. It is considered that the strength has decreased largely. There is a possibility that cracks or voids which become breakdown sources exist on the surface of the solidified body or in the interior thereof, which is the reason why the strength has decreased under these conditions. In this experiment, the surface was polished with sandpaper, and it was confirmed whether internal defects existed by X-ray CT and it was used for the test. However, it seems that scratches at the time of polishing and bubbles which can not be confirmed by visual inspection existed and these were sources of destruction. Another reason is that since the proportion of silica is large, the volumetric shrinkage rate at the time of reaction increased, and as a result, a large number of fine cracks entered the inside of the solidified body, so that the bending

strength decreased.

### **3.5 Conclusion**

From the results of this chapter, it was confirmed that the carbon nanoparticles/silica solidified body percolates with 40 vol.% of filler. Also, from the results of three-point bending test, the highest strength was at 20% of carbon nanoparticles. At this time, the strength was highest by preventing shrinkage as aggregate by carbon nanoparticles and making internal stress less likely to work. However, when increasing the amount of carbon nanoparticles to percolation concentration, the bond between silica was broken and the strength decreased. Observation by SEM revealed that a layer of carbon was formed around the silica particles.

The form of electrical conductive path should be an important point for improving electro-conductivity in ceramic composite. Thus, both amount and carbon material structure such as partical, graphite and carbon nanoparticles could be taken into consideration.

### **References**

- [1] T.T.T. Hien, T. Shirai, M. Fuji, An advanced fabrication route for alkali silicate glass by non-firing process. *Adv. Powder Technol.* 25(1) (2014) 360-364.
- [2] E.U. Apiluck, T. Shirai, K. Tomoaki, K. Orito, H. Watanabe, M. Fuji, M. Takahashi, Novel fabrication route for porous ceramics using waste materials by non-firing process, *J. Ceram. Soc. Jpn.* 118 (1380) (2010) 745-748.
- [3] G. Gorrasi, A. Sorrentino, Mechanical milling as a technology to produce structural and functional bio-nanocomposites, *Green Chem.* 17(5)(2015) 2610-2625.

- [4] T. Shirai, K. Orito, T.T.T. Hien, M. Fuji, Effects of different forming methods on the properties of solidified body by non-firing process through the mechanochemical treatment, *J. Jpn. Soc. Powder. Powder. Met.* 59 (9) (2012) 517-521.
- [5] M. Wakeshima, H. Masuda, K. Yamada, N. Sato, T. Fujino, New measurement system of specific resistivity and hall coefficient by four-probe van der pauw method, *Tohoku University* 52 (1/2) (1997) 135–144.

## **Chapter4 Effect of CNTs on Morphology and Electromagnetic Properties of Non-firing CNTs/silica Composite Ceramics: Fabrication and Application**

### **4.1 Introduction**

Since Iijima announced the first observation of carbon nanotubes, many studies have studied carbon nanotubes (CNTs) and developed a new research field for one-dimensional carbon nanomaterials [1]. Carbon nanotubes have excellent electrical properties [2,3], high compressive strength [4,5], thermal anisotropy [6-7], field emission characteristics [8] and other mechanical properties, as well as organic and inorganic Contaminants [9-11]. These properties have attracted the attention of researchers to synthesize carbon nanotube composites such as carbon nanotube/metal matrix composites [12], carbon nanotube/polymer matrix composites [13-17], and carbon nanotube reinforced ceramics composites [3,18-20]. In common synthetic materials, CNTs/ceramic composites were considered to increase electrical conductivity compared to the original ceramic material because even if the percolation threshold is very low, it could provide a continuous conduction path. Research through additions to ceramics as conductive fillers has focused mainly on adjusting the filler concentration to improve conductivity, and developed suitable fabrication methods that can maintain high aspect ratios, and CNTs nanostructures should always be considered one of them for CNT/ceramic composites. Material is the most important factor.

As we know, the high-temperature sintering process is a necessary and commonly used method for preparing ceramic materials to ensure high relative density. However, the sintering and calcination process not only consumes a large amount of

non-renewable energy, but also may cause harm to the environment such as carbon monoxide, sulfur dioxide and dust emissions. Even though spark plasma sintering (SPS) technology can effectively reduce the powder sintering temperature, it still needs to face high power consumption and high voltage [20]. In addition, especially for CNTs/ceramic composites, high sintering temperatures may affect the microstructure of carbon nanotubes, and to some extent hinder the chemical or mechanical properties of CNTs.

In order to solve these problems, the research team proposed an environmentally friendly ceramic material manufacturing method called non-firing process [21, 22]. The non-firing process means surface of the raw material ceramic powder is treated by a mechanical planetary ball mill [23], and the powder is continuously dispersed in an alkaline solvent [24] to form a precipitate, and finally a ceramic cured body is prepared. In addition, the manufacturing process should be performed at a much lower temperature (80 °C.) than the sintering process, thereby effectively achieving cost and energy reduction without requiring any other special sintering equipment.

By combining the carbon material with the SiO<sub>2</sub> ceramic matrix, this material is considered as the final reinforcement of the ceramic composite. In this study, we prepared CNTs/silica composite ceramics by non-firing process and investigated different volume fractions of CNTs on composite properties such as microstructure, morphology, mechanical behavior, electrical conductivity, and electromagnetic interference (EMI). Impact. Especially shielding at the Ku-band frequency.

## **4.2 Experimental section**

### **4.2.1 Materials and preparation**

A planetary ball mill with zirconia vials and zirconia balls ( $\Phi$ 1.5cm and  $\Phi$ 0.5cm)

was used to activate amorphous SiO<sub>2</sub> (SO-C1 prepared by VMC method, Admatechs Company Limited) at a rotation rate of 200 rpm, 15 minutes. The single-walled carbon nanotubes in this study were well-structured, with typical diameters in the range of 5-10 nm and ideal aspect ratios from Zeon Corporation. To prepare the ceramic composite, quartz powder (KS-100, F-plan) and raw CNTs were first mixed with a moderate amount of ethanol by 30 minutes sonication and a one-day tumbler ball mill. Next, for removing ethanol, the solution was dried to a powder by vacuum rotary evaporation. The presence of quartz during this process not only prevented the ceramic solid process from shrinking, but also disperses the CNTs into the solution.

The quartz/carbon nanotube composite powder was then mixed with the active SiO<sub>2</sub> and transferred to a resin tumbler with small zirconia balls for 4 hours to ensure good mixing of the material. After sufficient tumbler milling, a 1 mol/L KOH solution was added dropped to the powder to prepare ceramic slurry. Finally, the slurry was mixed with an electric mixer and then allowed to solidify at 80°C for 5 hours.

In order to investigate the effect of the amount of CNT on the ceramic composite, different carbon weight fractions in the mixed silica powder were prepared. The amounts of other components were listed in the Table. 4.1.

Table. 4.1. Component Volume and volume fractions of CNTs/silica composites.

Sample	Amorphous SiO <sub>2</sub>	Quartz	CNTs	1M KOH	
Component	(g)	(g)	(g)	wt. %	(g)
1	4.497	10.492	0.011	0.07	
2	4.493	10.485	0.022	0.15	2.88
3	4.487	10.469	0.044	0.30	
4	4.473	10.438	0.089	0.60	

#### 4.2.2 Characterization

Graphitization and structural defects of the carbon material at room temperature were measured using a Raman spectrometer (NRS-3100, JASCO Corporation). A transmission electron microscope (TEM) (JEM-2100F, JEOL Limited) observes the morphology of a ceramic body by a scanning electron microscope (SEM) (JSM-7000F, JEOL Limited). For the characteristics, electric conductivity was measured by the 4-probe Van der Pauw method [25]. Bending strength of the ceramic bulk was measured using a precision universal/tensile tester (AGS-G series, Shimadzu Corporation) having an average of 5 samples. The measurement progressed at 0.5% mm/min crosshead speed at room temperature and the dimensions of the sample were fixed to 0.5 cm × 1 cm × 5 cm (thickness × width × length). Electromagnetic interference reflecting ability was measured by the free space method of the frequency range of 8.2 to 110.0 GHz (microwave network analyzer, N5227A, Keysight Technologies).

### 4.3 Illustration and significance of non-firing ceramic process.

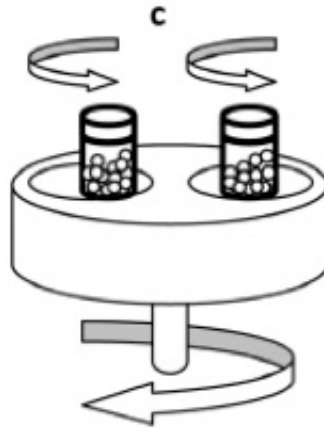


Fig. 4.1. Brief diagrammatic for planetary ball mill process.

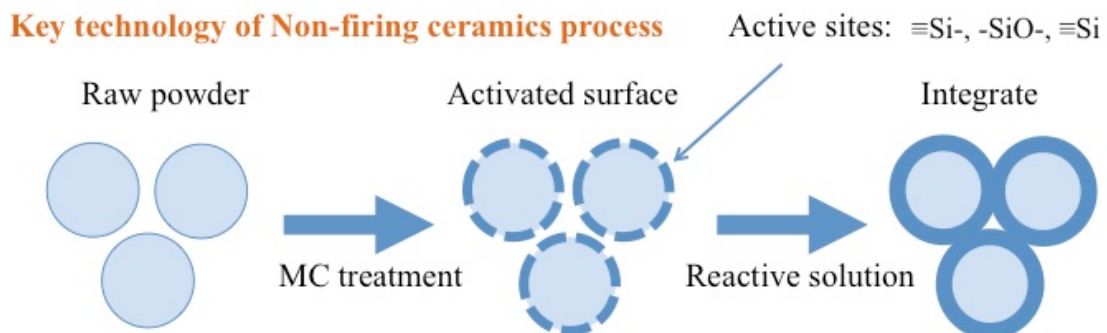


Fig. 4.2. Theoretic illustration of the non-firing ceramics preparation process from raw individual ceramic particle to ceramic body.

Comparing with traditional process of ceramic materials preparation, non-firing ceramic process has advantages in terms of facile fabrication, energy-saving, environmental friendly, and also low cost. There are two key factors for this method; first one is the mechanical treatment on the surface of the raw silica nanoparticles by a planetary ball-mill shown in Fig. 4.1. Adsorption of different compounds deposition on

the surface of silica-based materials are achieved during mechanical ball-mill. Siloxane bonding such as Si-O-Si, -Si-O- and  $\equiv\text{Si-}$  shown in Fig. 3.2 appear as chemical reactive ability sites [26]. Surface  $\equiv\text{Si-OH}$  groups can form as a result of rehydroxylation of dehydroxylated silica when the active silica is treated by alkaline aqueous solutions [27]. The surface silicon atoms tend to have a complete tetrahedral configuration; in addition, their free valence becomes saturated with hydroxyl groups in an aqueous medium [28]. After remove residual aqueous, silica particles bond with each other to form ceramic matrix with ensured mechanical property.

#### 4.4 Results and discussion

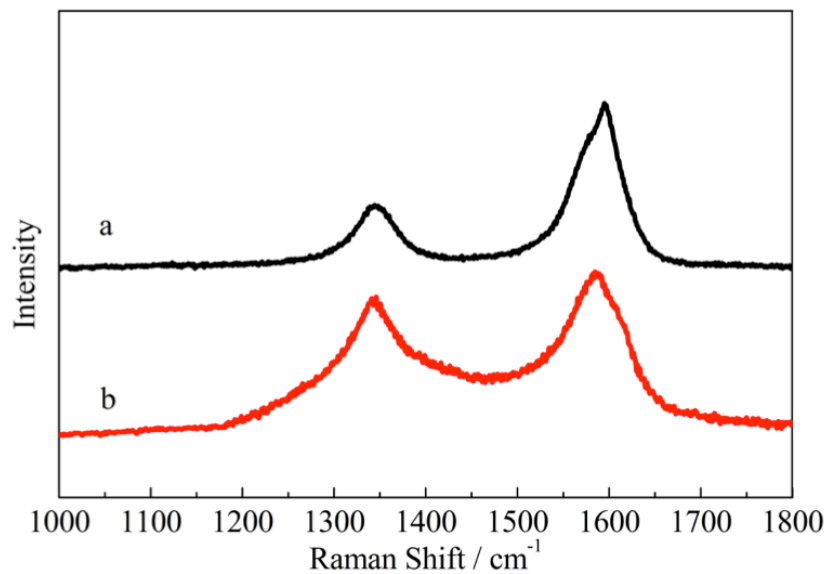


Fig. 4.3. Raman spectra of (a) raw carbon nanotubes and (b) silica-carbon nanotubes composite with 1.0 vol.% content of carbon nanotubes.

##### 4.4.1 Raman spectra

Raman spectra of raw CNTs and silica-carbon nanotube composites were measured and the present of carbon in the complex was examined (Fig. 4.3). The two characteristic bands of the carbon material are D-and and G-band respectively present in

the Raman shift of  $\sim 1350\text{ cm}^{-1}$  and  $1550\sim 1605\text{ cm}^{-1}$ . The D band is induced by disorder and defects [29], The G-band is an intrinsic feature associated with high level symmetry and well ordered carbon nanotubes and is closely related to the oscillation of all carbon materials formed by  $SP^2$  hybridization.

As shown in Fig. 4.3, both the raw CNTs and composite show a higher intensity of the G-band compared to the D-band. The R-value (intensity ratio of D-band to G-band) determines the degree of graphitization. After calculating, The R-value of raw CNTs ( $R_{\text{raw}} = 0.37$ ) is lower than that of silica-CNTs composite with 1.0 vol.% CNTs ( $R_{1.0} = 0.97$ ), which is mainly attributed to a symmetry-lowering effect due to defects, the presence of  $SiO_2$  nanoparticles, and also the amorphous carbon produced during the ball milling process [30,31]

#### 4.4.2 Morphology of composites

Figure 4.4 shows typical SEM images of a cross-sectional view of a CNTs-ceramic composite. By increasing the amount of CNTs from (a) 0.125 vol% to (b) 0.25 vol%, (c) 0.5 vol%, and (d) 1.0 vol%, it can be clearly observed from the figure that the carbon nanotubes effectively wrap around the network of carbon nanotubes is formed in the silica matrix and these carbon nanotubes provide interconnected conductive pathways in the composite. From the high magnification images (e) and (f) it can be seen that the sample exhibits three disordered structures; the heterogeneous polyhedral quartz in (e), the spherical silica nanoparticles combined with each other, and the diameter of about 10 nm in (f) tubular carbon material. These three structures intersected with each other.

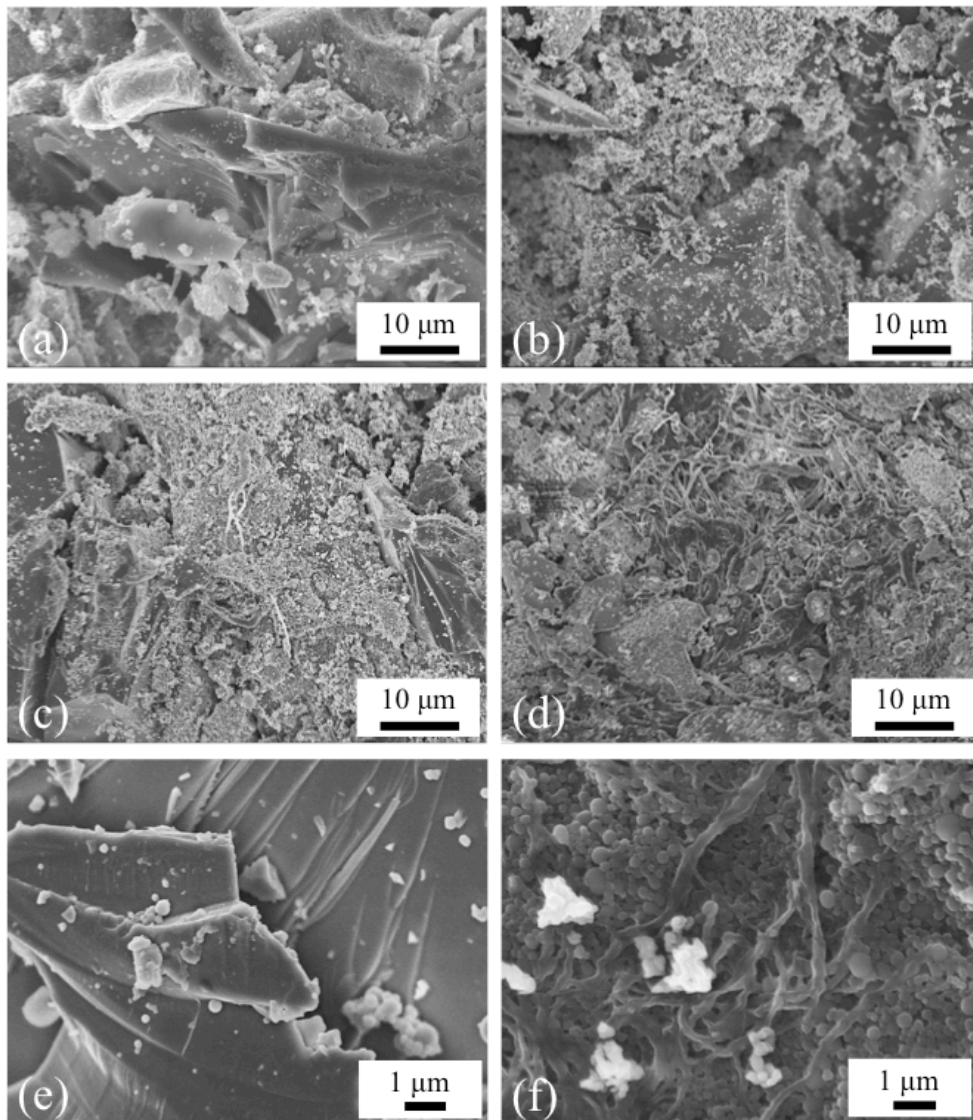


Fig. 4.4. SEM images of composite with different carbon nanotubes volume percentages from cross-section view. (a) 0.125 vol.% (b) 0.25 vol.% (c) 0.5 vol.% and (d) 1.0 vol.%. High magnification images of (e)(f) 1.0 vol.%

High magnification images of (e)(f) 1.0 vol.%

Concerning Fig. 4.4 (d), silica-carbon nanotube composites have a lower network density and a denser network microstructure. The composite material shows relatively uniformly dispersed carbon nanotubes in a silica matrix without affecting the formation and curing of the ceramic matrix. Meanwhile, after the non-fired preparation process, no

structure other than carbon material and nanotubes can function at lower temperatures compared to other copper processes.

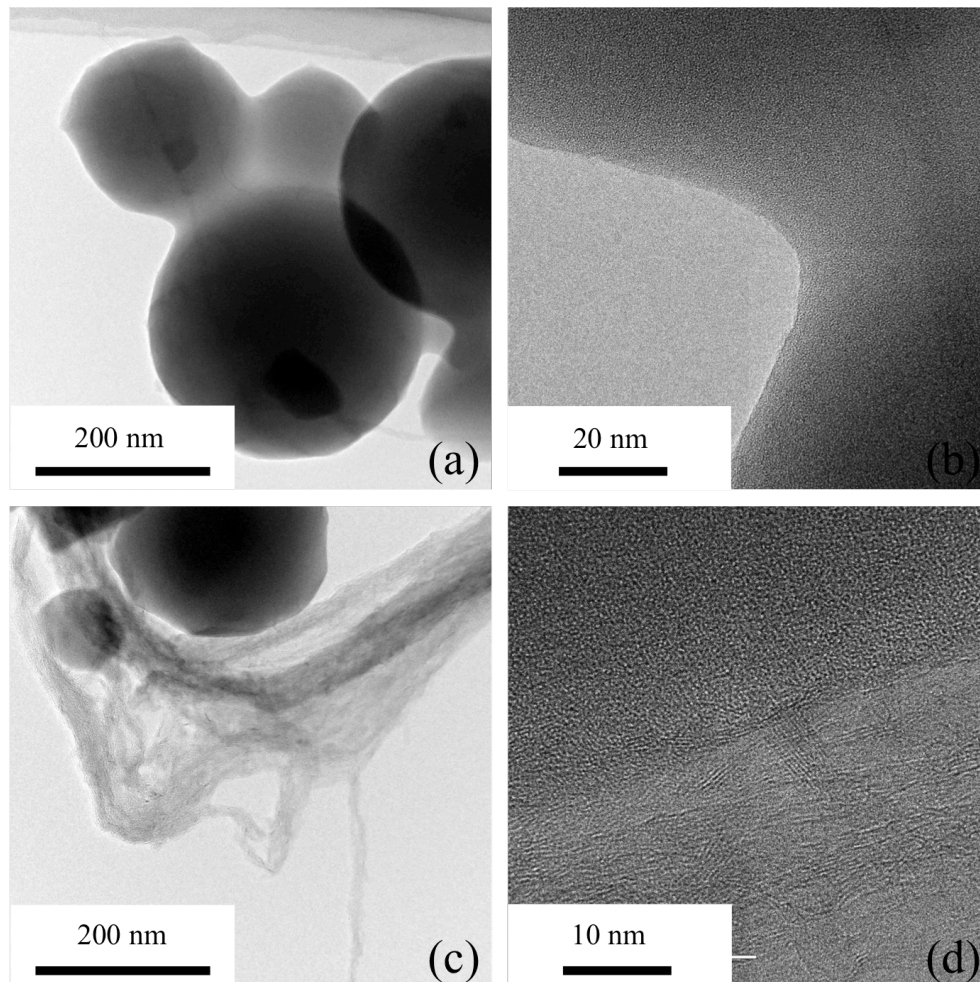


Fig. 4.5. TEM images of composite powders (a) combined structure between silica particles (low magnification) (b) (high magnification) and (c) boundary between CNTs- SiO<sub>2</sub> particles (low magnification) and (d) (high magnification).

Fig. 4.5 shows a TEM image of the combined structure between the interfaces ((c) and (d)) between silica particles ((a) and (b)) and CNTs-SiO<sub>2</sub> particles. As shown in Fig. 4.5 (a) and (b), after the addition of a certain amount of alkaline solution to the silica

-CNTs slurry, the raw spherical and inhomogeneous SiO<sub>2</sub> particles form a smooth internal combining with each other. The internal combination ensures the physical properties of the ceramic material. This morphology is highly consistent with the point that the planetary milling process leads to the appearance of an activation reaction mechanism, which means that the specific surface area of the amorphous silica powder [32] is increased in activity, and the slurry of the Si-rich pre-prepared powder passes the mechanical - the chemical activation treatment should effectively react with the alkaline solution and form new chemical bonds [33]. Concerning Fig. 4.5(c) and (d), intimate contact between the nanotubes and the silica composite structure was observed in the composite. During the formation of the silica continuum, the carbon material remains as a bundle and tube with a high long to length aspect ratio for determine the CNT network path structure.

#### 4.4.3 Electro and mechano properties.

The resistivity by the four-probe method and the mechano property by the three-point method are both shown in Fig. 4.6. The dependence of the amount of CNTs on the conductivity of the amount of silica/CNTs can clearly be observed.

The experimental results show that as the number of carbon nanotubes increases, the resistivity decreases, indicating that the formation of a conductive network contributes to ensuring that the electrons move freely in the material. After the carbon nanotubes were mixed into silica, the resistivity rapidly decreased from 4574.2 Ω·cm to 1244.1 Ω·cm, and finally reached 66.6 Ω·cm, within the semiconductor conductivity range. The threshold near the metal conductor was calculated as the conductivity [34, 35].

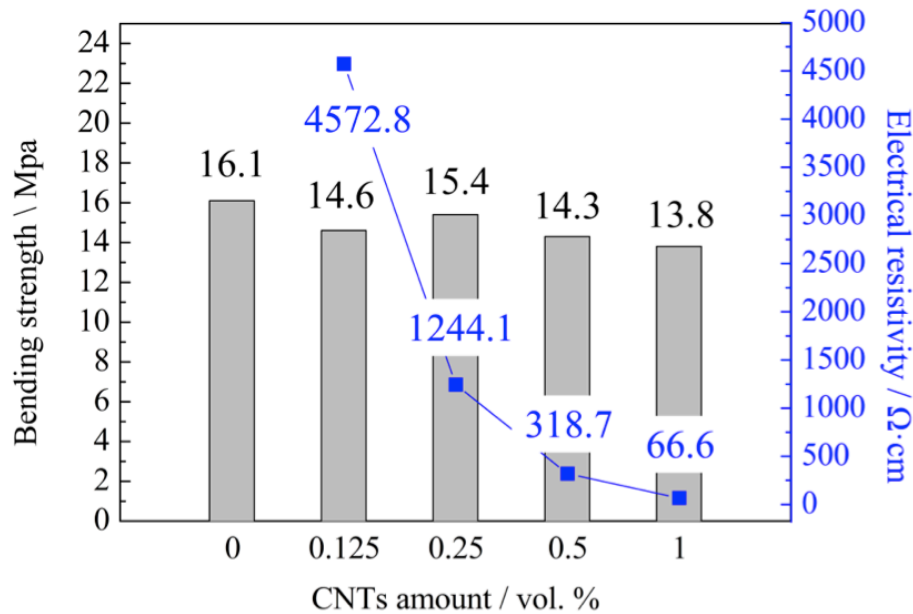


Fig. 4.6. Mechano and electro properties of composites with different CNTs amounts.

As the volume percentage of carbon nanotubes increases, the bending strength of the sample slightly decreases. It is considered that, compared with the non-CNTs ceramic material, since the interface between the carbon nanotube and the silica ceramic is weak, when the carbon nanotubes are added, the stress transfer inside the ceramic matrix will relax. With the increase in the volume percentage of carbon nanotubes in the composite, the agglomeration also increases, which affects the mechanical properties because it reduces the degree of densification of the sample.

Bending strength is an important parameter for both the ceramic material and ceramic composite. To develop more applications of composite ceramic material, focusing on improving the interface structure and reducing the porosity should be an effective method to improve the mechanical properties.

#### 4.4.4 EMI reflective ability.

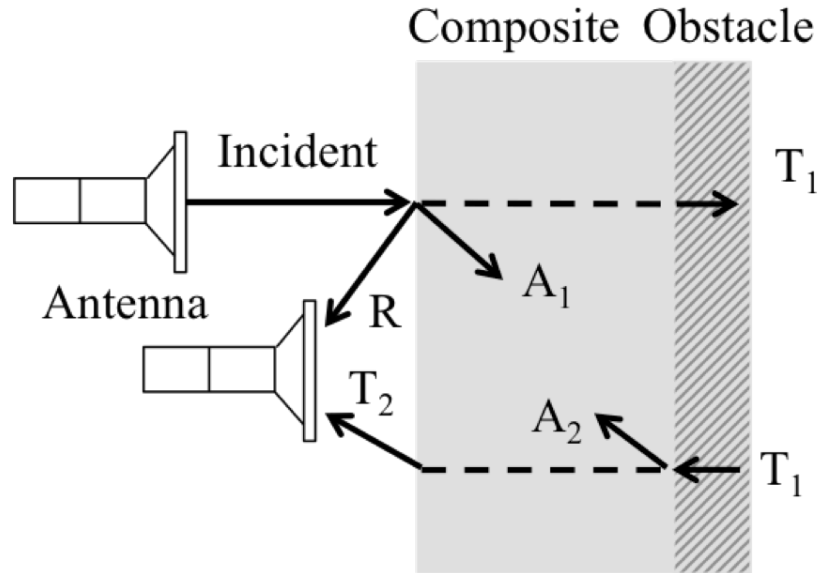


Fig. 4.7. Schematic of free space method

Since the free space method is a real and practical test for samples without requiring specific sizes and shapes, complete contact with a waveguide is also not required when compared to other methods [36]. As shown in Eq. (1), the power coefficient of the electromagnetic wave propagating in a material was described by the Transmissivity (T), Reflectivity (R) and Absorptivity (A) [37]. In order to simplify the discussion, multi-reflection will not be considered here.

$$T + R + A = 1 \quad (1)$$

A schematic diagram of the experimental method is shown in Fig. 4.7. The electromagnetic wave as an incident wave enters the samples vertically and separates into three parts: reflection (R), absorption (A<sub>1</sub>) and transmission (T<sub>1</sub>). Since a metal obstacle is located on the backside of the sample, it can be assumed that the

transmission part ( $T_1$ ) reflects into the sample again without any energy losses and reflection. The absorption and transmission occur again in the sample being abbreviated as  $A_2$  and  $T_2$ , respectively. The antenna setting in the vertical direction receives  $R$  and  $T_2$  finally and was directly measured using a network analyzer. In conclusion, Eq. (2) is a redaction on based on of Eq. (1) shown below:

$$(A_1 + A_2) + (R + T_2) = 1 \quad (2)$$

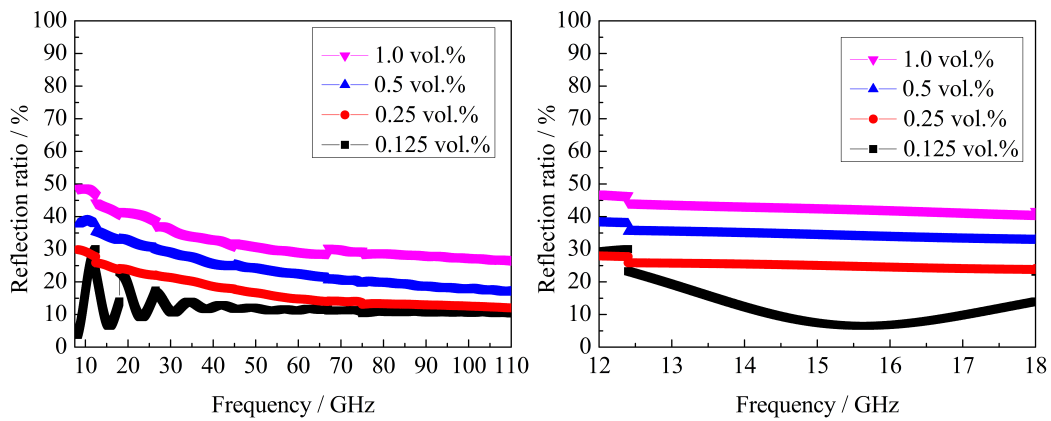


Fig. 4.8. Electromagnetic wave reflective ratio of CNTs/ceramic nanocomposites with different CNTs amounts.

In this work, the free-space method to evaluate the electromagnetic wave shielding ability of the CNTs/silica composite ceramics with different CNTs amounts. This measurement covers a wide frequency range from 8.2 to 110.0 GHz, and especially focusing on the frequency range from 12.0 to 18.0 GHz (Ku-band) shown in Fig. 4.8, which is used in the satellite communication field. Based on the results, the resonance of the absorption ratio occurs, which can be considered as the skin effect and the CNTs length to the incident wavelength. The absorption ratio also tends to be stable and as high as 90% has been achieved in the high frequency range. With the increase of CNTs

volume percentage, absorption ratio of ceramic composite shows a decreasing trend. Combined with Eq. (1), it can be considered that the ability of (R + T<sub>2</sub>) gradually increasing with the increase amount of the CNTs. The composites show structural applications as a kind of effective material in the EMI shielding research field.

#### **4.5 Conclusion**

In this work, combining mechano-chemical activation with a reactive solution, highly efficient and energy-saving processes for producing functional ceramics without firing and sintering processes have been proposed. By increasing the amount of CNT incorporated, a continuous path is effectively formed to produce the conductivity of the ceramic material. As the amount of carbon material increases, carbon nanotube/silica composite ceramics exhibit electromagnetic wave reflective ability.

In the present study, produced silica-based ceramic material still has a perfect type of properties, such as improved mechanical strength and EMI shielding capability. It should be taken into consideration that how to proposed and implemented a functional ceramic material more facile and more environmental-friendly methods in the future.

#### **References**

- [1] Iijima. S, Helical microtubules of graphitic carbon, *Nature* 354.6348 (1991) 56.
- [2] T.W. Ebbesen, H.J. Lezec, H. Hiura, J.W. Bennett, H.F. Ghaemi, Electrical conductivity of individual carbon nanotubes, *Nature* 382 (1996) 54-56.
- [3] S. Rul, F. Lefèvre-schlick, E. Capria, Ch. Laurent, A. Peigney, Percolation of single-walled carbon nanotubes in ceramic matrix nanocomposites, *Acta Mater.* 52 (4) (2004) 1061-1067.
- [4] P.M. Ajayan, L.S. Schadler, C. Giannaris, A. Rubio, Single-walled carbon nanotube–polymer composites: strength and weakness, *Adv. Mater.* 12 (10)

(2000) 750-753.

- [5] A. Chaipanich, T. Nochaiya, W. Wongkeo, P. Torkittikul, Compressive strength and microstructure of carbon nanotubes–fly ash cement composites, *Mater. Sci. Eng., A* 527 (4) (2010) 1063-1067.
- [6] A.M. Marconnet, N. Yamamoto, M.A. Panzer, B.L. Wardle, K.E. Goodson, Thermal conduction in aligned carbon nanotube–polymer nanocomposites with high packing density, *ACS Nano*, 5 (6) (2011) 4818-4825.
- [7] R.S. Ruoff, D.C. Lorents, Mechanical and thermal properties of carbon nanotubes, *Carbon* 33 (7) (1995) 925-930.
- [8] Q.H. Wang, T.D. Corrigan, J.Y. Dai, R.P.H. Chang, A.R. Krauss, Field emission from nanotube bundle emitters at low fields, *Appl. Phys. Lett.* 70 (24) (1997) 3308-3310.
- [9] A.H. Norzilah, A. Fakhru'l-Razi, Thomas S.Y. Choong, A.L. Chuah, Surface modification effects on CNTs adsorption of methylene blue and phenol, *J Nanomater* 55 (2011).
- [10] Y. Yao, F. Xu, M. Chen, Z. Xu, Z. Zhu, Adsorption behavior of methylene blue on carbon nanotubes. *Bioresour. Technol.* 101(9) (2010) 3040-3046.
- [11] C.Y. Kuo, Water purification of removal aqueous copper (II) by as-grown and modified multi-walled carbon nanotubes, *Desalin.* 249(2) (2009) 781-785.
- [12] C.D. Park, H.J. Jeon, H.J. Wang, Y.H. Choa, S.T. Oh, K.M. Kang, S.G. Kang, Synthesis of CNTs/Metal/Al<sub>2</sub>O<sub>3</sub> nanocomposite powders by chemical vapor deposition. *Mater. Sci. Forum* 449 (2004) 797-800.

- [13] H. Miyagawa, M. Misra, A.K. Mohanty, Mechanical properties of carbon nanotubes and their polymer nanocomposites, *J. Nanosci. Nanotechnol*, 5(10) (2005) 1593-1615.
- [14] X. Zeng, S. Yu, L. Ye, et al. Encapsulating carbon nanotubes with SiO<sub>2</sub>: a strategy for applying them in polymer nanocomposites with high mechanical strength and electrical insulation[J]. *Journal of Materials Chemistry C*, 2015, 3(1): 187-195.
- [15] L.Q. Zhang, B. Yang, J. Teng, et al. Tunable electromagnetic interference shielding effectiveness via multilayer assembly of regenerated cellulose as a supporting substrate and carbon nanotubes/polymer as a functional layer[J]. *Journal of Materials Chemistry C*, 2017, 5(12): 3130-3138.
- [16] S. Zhao, J. Li, D. Cao, et al. Percolation threshold-inspired design of hierarchical multiscale hybrid architectures based on carbon nanotubes and silver nanoparticles for stretchable and printable electronics[J]. *Journal of Materials Chemistry C*, 2016, 4(27): 6666-6674.
- [17] Y. Li, M. Li, M. Pang, et al. Effects of multi-walled carbon nanotube structures on the electrical and mechanical properties of silicone rubber filled with multi-walled carbon nanotubes[J]. *Journal of Materials Chemistry C*, 2015, 3(21): 5573-5579.
- [18] J. Ning, J. Zhang, Y. Pan, J. Guo, Fabrication and mechanical properties of SiO<sub>2</sub> matrix composites reinforced by carbon nanotube, *Mater. Sci. Eng., A*, 357 (1) (2003) 392-396.
- [19] Y. Yang, M.C. Gupta, K.L. Dudley, Studies on electromagnetic interference shielding characteristics of metal nanoparticle-and carbon nanostructure-filled

- polymer composites in the Ku-band frequency. *Micro. Nano Lett.* 2 (4) (2007) 85-89.
- [20] S.L. Shi, J. Liang, The effect of multi-wall carbon nanotubes on electro magnetic interference shielding of ceramic composites. *Nanotechnology*, 19 (25) (2008) 255707.
- [21] T.T.T. Hien, T. Shirai, M. Fuji, An advanced fabrication route for alkali silicate glass by non-firing process. *Adv. Powder Technol.* 25(1) (2014) 360-364.
- [22] E.U. Apiluck, T. Shirai, K. Tomoaki, K. Orito, H. Watanabe, M. Fuji, M. Takahashi, Novel fabrication route for porous ceramics using waste materials by non-firing process, *J. Ceram. Soc. Jpn.* 118 (1380) (2010) 745-748.
- [23] G. Gorrasi, A. Sorrentino, Mechanical milling as a technology to produce structural and functional bio-nanocomposites, *Green Chem.* 17(5)(2015) 2610-2625.
- [24] T. Shirai, K. Orito, T.T.T. Hien, M. Fuji, Effects of different forming methods on the properties of solidified body by non-firing process through the mechanochemical treatment, *J. Jpn. Soc. Powder. Powder. Met.* 59 (9) (2012) 517-521.
- [25] M. Wakeshima, H. Masuda, K. Yamada, N. Sato, T. Fujino, New measurement system of specific resistivity and hall coefficient by four-probe van der pauw method, *Tohoku University* 52 (1/2) (1997) 135–144.
- [26] L. Teokcharov, D. Simeonov, I. Uzunov, D. Klissurski, Mechanochemical modification of silica, *J. Mat Sci. Let.*, 11 (1992) 1180-1182.
- [27] H.T.T.Thu, T. Shirai, M. Fuji, An advanced fabrication route for alkali silicate glass by non-firing process, *Adv. Powd. Technol.*, 25 (1)(2014) 360-364.

- [28] L.T. Zhuravlev, Surface characterization of amorphous silica-a review of work from the former USSA, *Colloid. Surf. A: Physicochem. Eng. Aspects*, 74 (1993) 71-90.
- [29] M.S. Dresselhaus, G. Dresselhaus, A. Jorio, A.G. Souza Filho, R. Saito, Raman spectroscopy on isolated single wall carbon nanotubes, *Carbon* 40 (12) (2002) 2043-2061.
- [30] K.E. Thomson, D. Jiang, R.O. Ritchie, A.K. Mukherjee, A preservation study of carbon nanotubes in alumina-based nanocomposites via Raman spectroscopy and nuclear magnetic resonance. *Applied Physics A*. 89 (3) (2007), 651-654.
- [31] D. Jiang, K. Thomson, J.D. Kuntz, J.W. Ager, A.K. Mukherjee, Effect of sintering temperature on a single-wall carbon nanotube-toughened alumina-based nanocomposite. *Scripta Mater.* 56 (11) (2007) 959-962.
- [32] T.T.T. Hien, T. Shirai, M. Fuji, Mechanical modification of silica powders, *J. Cera. Soc. Jpn.* 120 (1406) (2012) 429-435.
- [33] W.K.W. Lee, J.S.J. van Deventer, Chemical interactions between siliceous aggregates and low-Ca alkali-activated cements, *Cem. Concr. Res.* 37 (6) (2007) 844-855.
- [34] J.F. Shackelford, M.K. Muralidhara, *Introduction to materials science for engineers* (2005).
- [35] G.D. Zhan, A.K. Mukherjee, Carbon nanotube reinforced alumina-based ceramics with novel mechanical, electrical, and thermal properties, *Int. J. Appl. Ceram. Tec.* 1 (2) (2004) 161-171.
- [36] S. Geetha, K.K. Satheesh Kumar, C.R Rao, M. Vijayan, D.C. Trivedi, EMI shielding: methods and materials-a review, *J. Appl. Polym. Sci.* 112 (4) (2009)

2073-2086.

- [37] S. Kwon, R. Ma, U. Kim, H.R. Choi, S. Baik, Flexible electromagnetic interference shields made of silver flakes, carbon nanotubes and nitrile butadiene rubber, *Carbon* 68 (2014) 118-124.



## **Chapter5 Effect of Silane Modification on CNTs/silica to Enhance Composites Interfacial Property and Dispersibility**

### **5.1 Introduction**

As a kind of one-dimensional structural carbon material, carbon nanotubes (CNTs) raised increasing interests for researchers [1,2] pushing its outstanding properties to varies applications as possible with other types of different materials such as metal [3,4], polymer nanocomposite [5,6], resin and ceramic matrix [7-10]. The outstanding electrical conductivity [11,12], extensive mechanical [13,14] and optical [15] property, thermal stability [16] as well as unique energy-saving ability [17] gave a great diversity of possibility to its potential applications. Thus, CNTs filled composites were investigated in the area of CNTs composite materials in recent years.

Common effective methods to improve kinds of properties are: surface modification on CNTs such as oxidation and deposition characterization [18,19]; adding surfactant [20]; in-site synthesis [21]; as well as applying methods of silane coupling agents [22,23]. Among them, oxidation on nanotubes surface plays an important role in the modification of CNTs [13,24,25]. During modification, the hydroxyl and carboxyl groups that are introduced in the oxidation process can be used for further reacting with other chemical agents. The functionalized carbon nanotubes (CNTs) are widely applied as additives for structural composite materials adding carbon nanotubes and amino compounds with hydroxyl groups, especially in polymer and ceramic hosting matrix [26]. For conclusion, chemical interfacial bonding, random dispersibility to against ubiquitous high surface energy in nano scaled materials, and tube structure retainability are three major challenges and key factors for CNTs filled composite materials as

further development tendency.

Moreover, in the process of ceramic fabrication, high-temperature sintering is a necessary and common method, which could ensure a high relative density. However, both the sintering and calcination processes consuming large amounts of non-renewable energy resources, and also possibly doing harm to the environment such as CO, SO<sub>2</sub> and dust emissions during the process [27]. Even if the spark plasma sinter (SPS) technology can effectively reduce the powder sintering temperature, it still has to be faced with a high power consumption and high pressure [28]. Especially for the CNTs/ceramic composite, the high sintering temperature may impacts the carbon material nanotube microstructure and hampers the CNTs chemical or mechanical properties to some extent. In order to solve these problems, a non-firing process was proposed as an environmental-friendly ceramic material fabrication method [29,30]. Non-firing process means treating the surface of raw ceramic powder by mechanical planetary ball mill activation [31], then continuously dispersing powder in an alkaline solvent [32] to form precipitates. Eventually, prepare ceramics solidified body. In addition, the fabrication processes could proceed at a much lower temperature (80°C) than the sintering method, so that it effectively achieves reducing cost and energy without requiring any other special sintering equipment.

On this basis, one kind of silane coupling agent, 3-aminopropyl triethoxysilane (APTES) in synthetic materials with silica nanoparticles as typical additives, was chosen since the amino group and the alkoxy groups on both sides of APTES molecule chain bonded to the silicon atom ensure chemical bonding with pre-treated CNTs [33,34] and silica particles [35]. APTES functionalized CNTs adding into silica not only improved the physical combining of two materials to chemical bonding but also

promoted the dispersibility of CNTs to resist its agglomeration since high surface energy as nano material. APTES was stable and remaining activity in the alkaline atmosphere [36], which was precisely adapted to non-firing process. Thus, an improvement on dispersibility, interfacial bonding and processing has been proposed in this work to fabricate silica-APTES-CNTs functional composite material.

## 5.2 Experimental section

### 5.2.1 Materials

SiO<sub>2</sub> (SO-C1 by VMC method, Admatechs Co., Ltd) was mechanically treated by ZrO<sub>2</sub> balls and vials (under the condition of 200 r/m, 15 min) firstly in order to used as one of the ceramic body materials. Polyhedral quartz powder (KS-100s, F-plan) was also chosen as another body material. Multi-walled CNT (VGCF-H, Showa Denko) with an average fiber length of 10~20 μm and diameter of 150 nm was used as the added fillers. Silane coupling agent 3-aminopropyl triethoxysilane (APTES, obtained from Shin-Etsu Chemical Co., Ltd. KBE-930) and mixed acid H<sub>2</sub>SO<sub>4</sub>:HNO<sub>3</sub> = 3:1 (Kanto Chemical Co., Inc. and Wako Pure Chemical Industries, Ltd. Respectively) were used to modify the surface chemical environment of MW-CNTs.

### 5.2.2 Preparation process

At first, 2g as-received MW-CNTs was acid-treated by 90 mL H<sub>2</sub>SO<sub>4</sub> and 30 mL HNO<sub>3</sub>. In details, CNTs was added into mix acid and slightly stir by a glass rod. Then pulled the solution slowly into a three-necked flask for water bath during 6 hours under 80°C. After water bath process, the solution was filtered through distilled water by times until PH value reaching neutral. The aqueous solution was dried at 60°C overnight to obtain the acid-CNTs powder for further APTES functionalization. Take a quota of APTES to solute in ethanol then stirring for 2 hours under room temperature before

adding pre-treated acid-CNTs into solution. The APTES and Acid-CNTs were sufficiently reacted with each other during string section and finally dried to powder named APTES-CNTs. Amorphous SiO<sub>2</sub> was mechanical treatment to obtain active sites on surface by planetary ball mill (Pulverisette.5, Frisch Japan Co. Ltd.) at first, and then a moderate amount of quartz was well mixed with activated SiO<sub>2</sub> to form the silica ceramic matrix material after 4 hours tumbler ball milling with small size of zirconia balls. After sufficient tumbler ball milling, silica powder was transferred into a plastic bottle for further fabrication with APTES-CNTs. For ceramic composite fabrication, all the components were mixed together follow gradually increased CNTs volume percentages. Then 2.88 g 1 mol/L KOH solution was dropped to mixed powder to prepare the ceramic slurry by an electric mixer (ARV-930TWIN, THINKY), which could both mix and deform slurry. At last, obtained slurry was immediately poured into a mold keeping 5 hours at 80°C for solidification. To investigate the effect of the CNTs amount on the ceramic composite, different carbon concentrations from 0.25%, 0.5%, 0.75%, 1.0%, 4.0% and 6.0% in the blended silica powder were prepared.

### 5.2.3 Characterizations

Raman spectrometer NRS-3100 Laser Raman Spectrophotometer (excitation source of 523nm wavelength) produced by JASCO Corporation was used to determine the phase compositions at room temperature. FT-IR spectrum was recorded by JASCO Corporation FT/IR-6200 Fourier Transform Infrared Spectrometer with KBr pellets. The X-ray photoelectron spectroscopy (XPS) of samples were obtained using the ESCALAB 250, Thermo Fisher Scientific USA with the 150W scanning X-ray source of monochromated Al kalph. SEM observation was applied at an accelerating voltage of 10kV by a JEOL JSM-7600F field emission scanning electron microscope. Three-point

bending strength was measured by SHIMADZU AGS-G Series Universal/Tensile Tester with a constant pressure of 5 KN.

### 5.3 Results and discussion

#### 5.3.1 Raman spectra

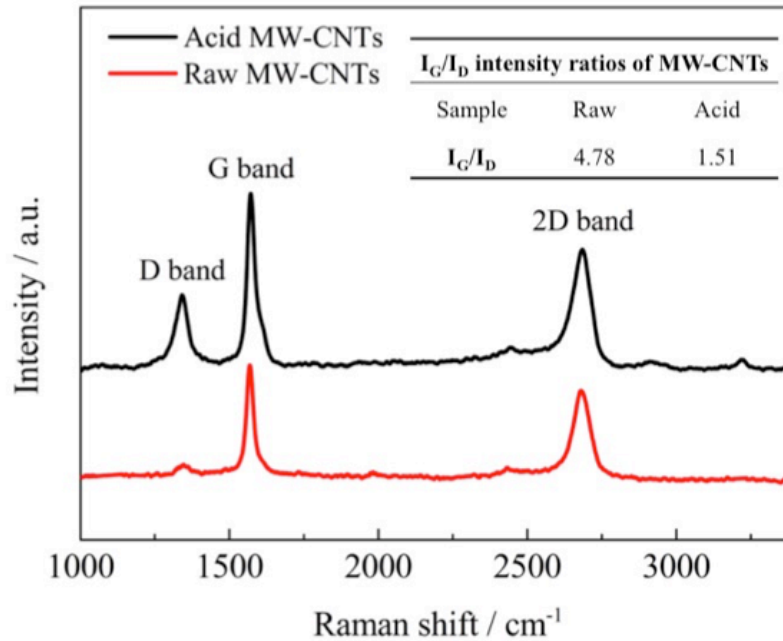


Fig. 5.1 Raman spectra and  $I_G/I_D$  intensity ratios of raw and acid treated MW-CNTs.

Raman spectra of as-received raw and  $H_2SO_4/HNO_3$  treated MW-CNTs are shown in Fig. 4.1. Both of them consist of three typical bands, respectively named the D-band ( $\sim 1342cm^{-1}$ ), G-band( $\sim 1572cm^{-1}$ ) and 2D-band( $\sim 2684cm^{-1}$ ) [37]. D-band originated from the existence of amorphous carbon and disordered structure rather than seamless concentric tube structure formed by carbon atoms in the hexagonal arrangement. Defects of CNTs concentrate represent as vacancies of carbon atoms, heptagon instead of hexagon, and also kinds of functional groups modification on surface. G-band corresponding to the graphite structure of CNTs. The peak of 2D-band is the second order of the D-band peak, which is caused by the double resonant Raman scattering,

involved by two-phonon emissions with opposite momentum.

From Fig. 5.1, it is obvious that an increase of the D-band has occurred intensively after acid treatment when comparing with raw CNTs. To calculate the corresponding ratio of D-band and G-band characteristic peak intensity ( $R=I_D/I_G$ ) showing in Fig. 5.1, a significant reduction of the R-value from 4.78 to 1.51 was estimated. Combining to functionalization process of mix acid to CNTs, it can be concluded that functional groups such as -COOH and -OH were introduced to affect the carbon  $sp^3$  hybrid structure during acid treatment, and also carbon defect on both walls and tips of CNTs. 2D-band revealed a slightly hypsochromic shift to higher vibration energy, since the stress effect when structure disturbed by defects and disorder.

### 5.3.2 FT-IR spectrum

Fig. 5.2 shows the FT-IR spectra of raw MW-CNTs, oxidized MW-CNTs, and also the reaction product of silica-APTES-CNTs. Raw multi-walled CNTs spectrum reveals peak at wave number of  $1575\text{cm}^{-1}$  and  $2361\text{ cm}^{-1}$  are attributed to the presence of conjugated C=C stretching and the  $\text{CO}_2$  in the atmosphere. Spectrum of MW-CNTs after oxidization by mix acid not only shows the  $1575\text{ cm}^{-1}$  attributing to C=C stretching of raw material but also the appearance of and absorption band at  $1720\text{ cm}^{-1}$ . This could be assigned to stretching vibrations of carboxylic groups -COOH as a consequence of acid treatment process on raw CNTs.

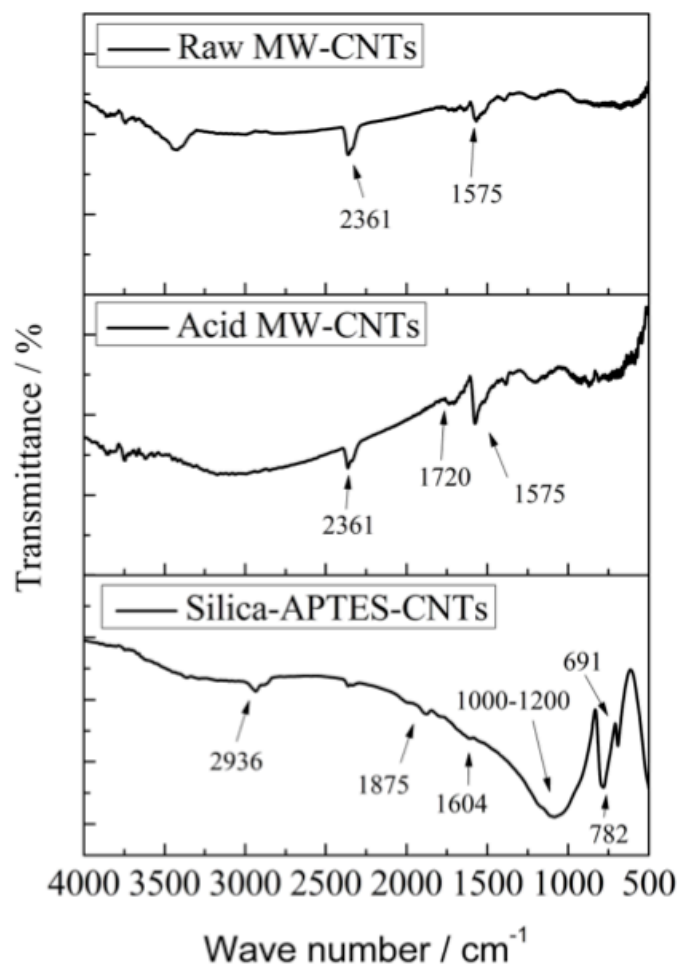


Fig. 5.2. FT-IR spectrum of raw MW-CNTs, acid treated MW-CNTs and APTES functionalized MW-CNTs reacted with silica nanoparticles.

FT-IR spectrum of the APTES surface functionalized MW-CNTs reacted with silica is also presented in Fig. 5.2. It shows that the characteristic peaks at  $2936\text{ cm}^{-1}$ ,  $1640\text{ cm}^{-1}$ , and band range of  $1000\text{-}1200\text{ cm}^{-1}$  are corresponding to the stretching of N-H groups, C-N stretching of amide functional group and additional bands such as Si-O-R asymmetric stretching vibration and Si-C or Si-OH deformation vibrations which grafting to acid MW-CNTs, respectively. The two new peaks attributed from

APTES or APTES reacted with acid MW-CNTs as expected. Peaks present at  $691\text{ cm}^{-1}$  and  $782\text{ cm}^{-1}$  attributed to Si-O-Si stretching and Si-OH functional groups of surface active hydroxylate silica nanoparticles. A disappearance of peaks presented at  $1720\text{ cm}^{-1}$  can be also observed in the figure of silica-APTES-CNTs, which further indicated -COOH functional group on the surface of acid-treated CNTs was reacted with -NH group in APTES to combine as C-N [38].

Comparing the FT-IR spectrums of raw multi-walled CNTs, Acid-treated CNTs and silica-APTES-CNTs, the successful reaction of silica with APTES functionalized acid MW-CNTs was evidenced by above spectrums.

#### 4.3.3 Composite morphologies from cross-section view

Typical Scanning electron microscopy images of the CNTs/ceramic composites from cross-section view under low magnification are shown in Fig. 5.3 (a) (c) and high magnification in (b) (d). The morphology changes of CNTs in ceramic matrix were detected since APTES modification. It can be seen from the Fig. 5.3 (a) (c) that samples presented three types of disorderly structures intersected with each other: inhomogeneous polyhedron quartz, spherical silica nanoparticles combined with each other, and carbon nanotubes remain as received dispersing in matrix. Morphology of silica-APTES-CNTs composite in Fig. 5.3 (b) shows a high CNTs dispersibility and it is effectively entangled into the silica matrix. Moreover, it can be clearly observed that most of the CNTs remain intact even after APTES functional treatment and only the end parts of nanotube rope suspend on surface of silica, while CNTs in silica-acid CNTs composite was aggregated (circled and pointed out) in Fig. 5.3(c) and pulled out from silica matrix in Fig. 5.3 (d).

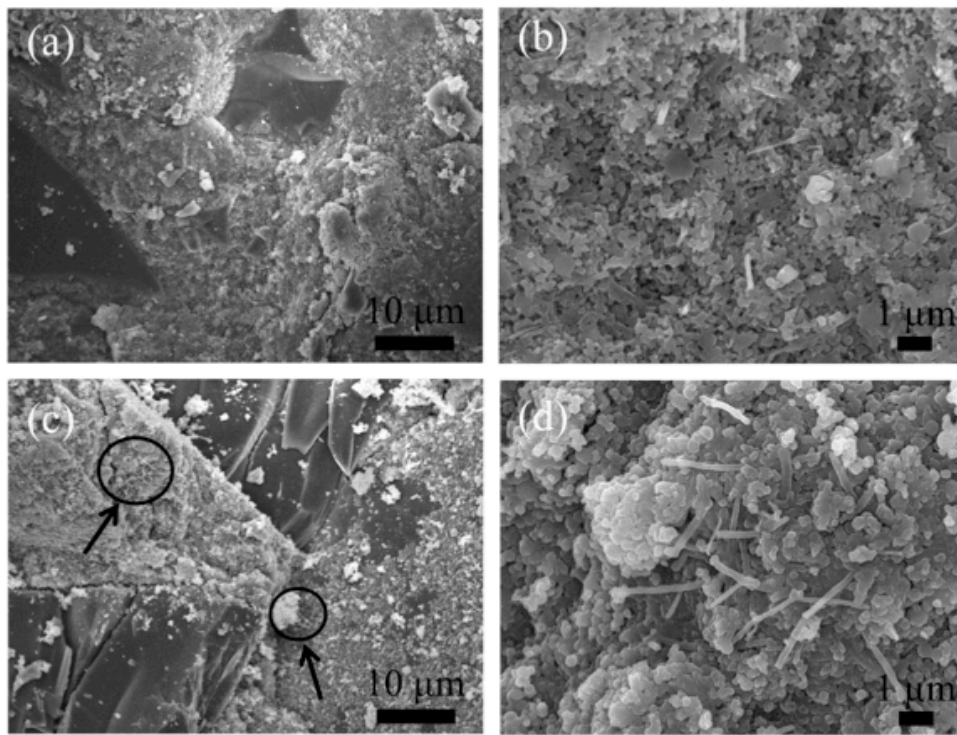


Fig. 5.3 Typical Scanning electron microscopy images of the CNTs/ceramic composites from cross-section view under low magnification are shown in Fig. 5.3 (a) (c) and high magnification in (b) (d).

### 5.3.4 XPS and bending strength

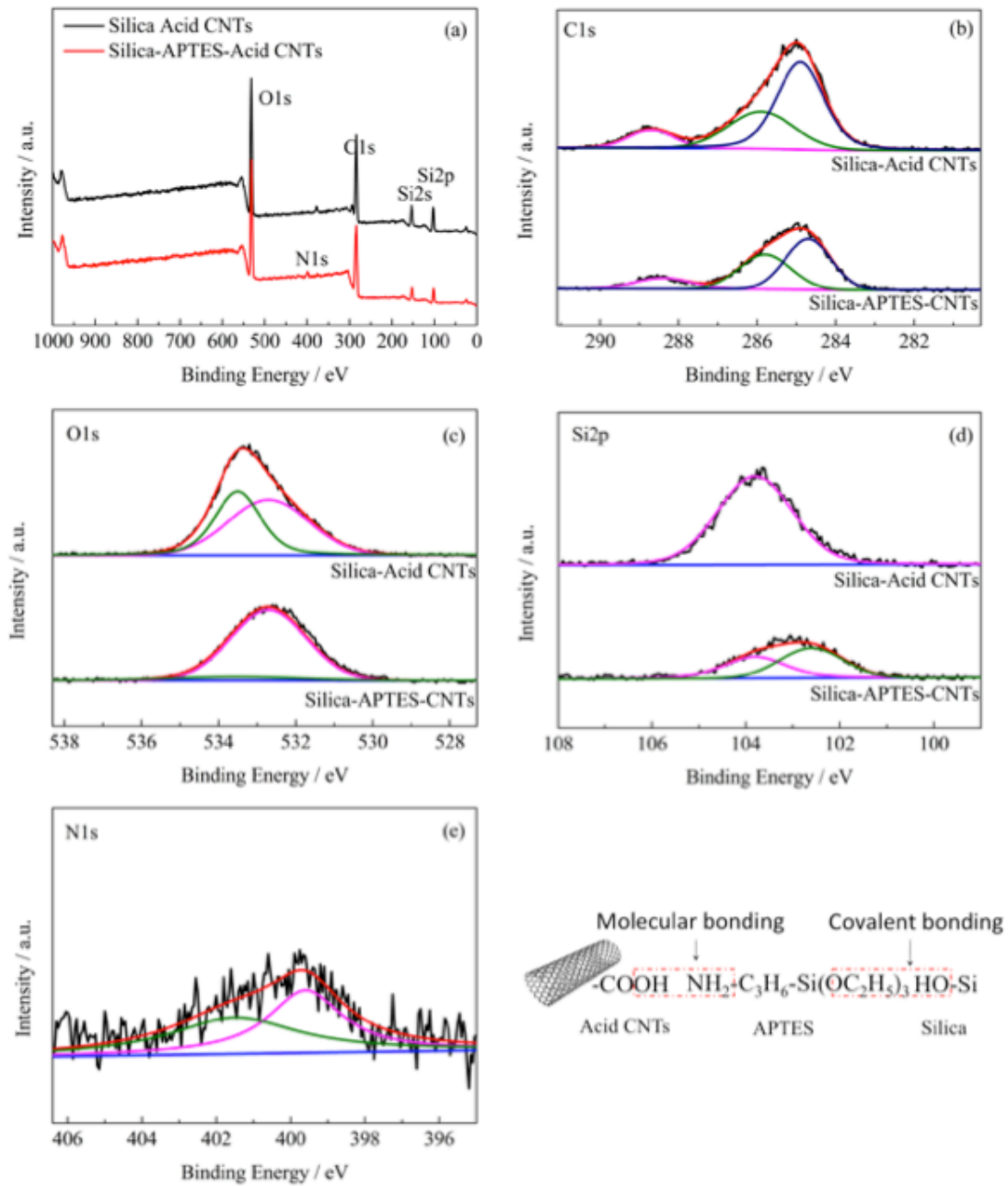


Fig. 5.4. XPS spectra of silica-acid CNTs and silica-APTES-CNTs (a) total of elements, (b) C1s, (c) O1s, (d) Si2p and (e) N1s spectra of silica-APTES-CNTs and Illustration of composite.

Table. 5.1. XPS analysis summary results of MW-CNTs added silica ceramic with/without APTES functionalized.

Sample	O1s		C1s			Si2p		N1s		
	BE/eV	533.5	532.7	288.4	285.8	284.7	103.8	102.6	401.5	399.6
Silica-Acid	at%	15.8	13.7	5.8	16.3	24.0	23.3	-	-	
CNTs	Total%	29.5		46.2			23.3		-	
Silica-APTES-	at%	1.6	32.0	4.3	18.6	36.8	5.5	7.6	2.3	2.6
CNTs	Total%	33.6		56.6			13.0		4.9	

X-ray photoelectron spectroscopy (XPS) is a kind of surface analytical techniques to study chemical information of functional groups. To determine elements presence on the surface or structure defects of CNTs, XPS spectra of main element, C1s, O1s, Si2p, and N1s were shown in fig. 5.4. Summary of core-level binding energy (BE) and atomic% for main surface atoms in Table 5.1 provided specific information of silica-acid CNTs and silica-APTES-CNTs.

Upon the deconvolution C1s peak both in the spectra of silica-acid CNTs and silica-APTES-CNTs composites, the main peak at 284.7 eV was observed, apparently attributed to the graphite characteristic structure of carbon nanotube. Moreover, peak at 285.5 eV attribute to different oxygen-containing hydroxyl groups, which can be regarded as defects on the nanotubes. Finally a weak peak at 288.3 eV attached to carbon atoms involved in two oxygen such as carboxyl (-COOH), carboxylic anhydrides and ester.

Since APTES functionalized CNTs before composite with silica, the C-O at 285.5

eV was slightly increased to provide the absence of APTES [39]. Furthermore, peaks at both 284.7 eV and 288.3 eV tend to show binding energy decrease (atomic% of C1s Table 5.1), according to APTES amino group react with -COOH on surface of CNTs. Above of C1s peak variation indicated the successful chemical surface bonding of APTES to acid CNTs.

Deconvolution of the O1s peak from silica-acid CNTs composite spectrum results in two peaks at and 532.7 eV and 533.5 eV, which can be attributed to O=C oxygen atoms double bond in aldehyde and ketone moieties and O-C single bond both involved in ethers and hydroxyl function groups, respectively. For composite of silica-APTES-CNTs from fig. 5.4(c), A significant increment can be observed at peak of 533.5 eV. Table 5.1 enumerates O1s atomic% of O-C bound increasing from 13.7% in acid oxidized CNTs composite to 32.0% in APTES functionalized CNTs composite. The intensity of peak decreased mainly attribute to the addition of silane coupling agent to introduce oxygen atoms bonded to silicon in APTES molecule. In addition, since the presence of alkoxy functional groups, Si-O-C bond provided more oxygen single bond in composite [35].

Si2p band of silica-acid CNTs which was deconvoluted into a Si-O peak at 103.8 eV, attributing to silicon-oxygen bond in raw silica material. While beside the peak at 103.8 eV, an additional peak appeared in APTES functionalized composite at 102.6 eV apparently due to the existence of silicon atoms bond to alkoxy (Si-O-C) in APTES molecule. Atomic% of Si2p in Table 5.1 specifically shows an appearance at 102.6 eV after APTES modification [40]. Fig. 5.4(e) presents two peaks of N1s for silica-APTES-CNTs composite respectively at 399.6 eV and 401.5 eV, corresponding to amide and amide group in silane coupling agent reacted with carboxyl acid group on

oxide CNTs surface. No peak appeared in silica-CNTs for N1s since the absence of APTES modification [38].

In conclusion, results from XPS confirm that the surface of acid multi-walled CNTs was successfully modified by APTES with reacting acidic groups to amino groups, whereas covalent bonding between the alkoxy from APTES and hydroxyl functional groups were generated to further combining CNTs/silica composite with silane coupling agent. Results are high accordant with FT-IR and SEM data, indicating an effective interfacial bond enhancement between materials.

### 5.3.5 Composite bending strength property

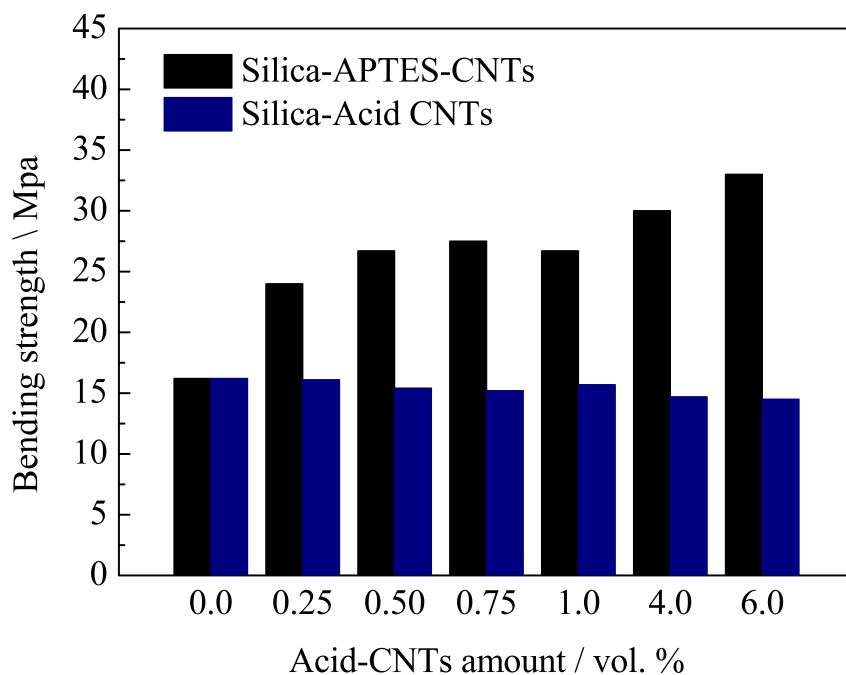


Fig. 5.5. Bending strength of silica-acid CNTs and silica-APTES-CNTs with different CNTs vol.%.

Fig. 5.5 shows the bending strength of silica-acid CNTs and silica-APTES-CNTs with increase volume percentage of CNTs. It can be suspected that compare with

ceramic matrix without APTES treating, silica-APTES-CNTs composites shows a higher bending strength to silica-acid CNTs composites under all ratios. This is due to the molecular and covalent chemical bonding respectively between acid nanotube/APTES and APTES/silica. Also, with the addition of APTES functionalized carbon nanotubes from 0.25 vol.% to 6.0 vol.%, reaction between ceramic matrix and multi-walled CNTs trend to be more effective for enhancing mechanical properties. Bending strength is an important parameter for both the ceramic material and ceramic composite, in this case, focusing on improving the interface structure and decreasing the porosity should be an effective method to increase the mechanical properties.

#### **5.4 Conclusion**

In the present work, an efficient and energy-saving process was proposed to fabricate CNTs/silica ceramic composite without any calcination and sintering processes by the effect of mechano-chemical activation and reactive solution. Addition of silane functionalization on carbon nanotube surface is investigated on the interfacial bonding, dispersion and mechanical properties of epoxy composites with different contents of CNTs. Results showed that amino and alkoxy groups on both sides of APTES molecule were respectively chemically bonded with oxidized CNTs and surface activated silica nanoparticles. It has also been proven that bending strength of CNTs/silica composites were increased under the influence of different CNTs amounts. These can be the basis to provide a method for further research on improving the mechanical property and thermal stability to achieve a variety of applications on ceramic based CNTs nanocomposites.

## References

- [1] M. Terrones, Science and technology of the twenty-first century: synthesis, properties, and applications of carbon nanotubes, *Annual review of materials research*. 33 (2003) 419-501.
- [2] M.F.L. De Volder, S.H. Tawfick, R.H. Baughman, A.J. Hart, Carbon nanotubes: present and future commercial applications, *Science*. 339 (2013) 535-539.
- [3] X.X. Zhang, H.M. Wei, A.B. Li, Y.D. Fu, L. Geng, Effect of hot extrusion and heat treatment on CNTs-Al interfacial bond strength in hybrid aluminium composites, *Compos. Interface.*. 20 (2013) 231-239.
- [4] C.D. Park, H.J. Jeon, H.J. Wang, Y.H. Choa, Synthesis of CNTs/Metal/Al<sub>2</sub>O<sub>3</sub> nanocomposite powders by chemical vapor deposition, *Mater. Sci. Forum*. 449(2004)797-800.
- [5] H. Miyagawa, M. Misra, A.K. Mohanty, Mechanical properties of carbon nanotubes and their polymer nanocomposites, *J. Nanosci. Nanotechnol.* 5 (2005) 1593-1615.
- [6] X. Zeng, S. Yu, L. Ye, M. Li, R. Sun, Encapsulating carbon nanotubes with SiO<sub>2</sub>: a strategy for applying them in polymer nanocomposites with high mechanical strength and electrical insulation, *J. Mater. Chem. C*. 3 (2015) 187-195.
- [7] S. Bi, L. Ma, B. Mei, Q. Tian, C.H. Liu, C.R. Zhong, Y.D. Xiao, Silicon carbide/carbon nanotube heterostructures: controllable synthesis, dielectric properties and microwave absorption, *Adv. Powder Technol.*. 25 (2014) 1273-1279.

- [8] S. Rul, F. Lefèvre-schlick, E. Capria, C. Laurent, Percolation of single-walled carbon nanotubes in ceramic matrix nanocomposites, *Acta Mater.* 52 (2004) 1061-1067.
- [9] J. Ning, J. Zhang, Y. Pan, J. Guo, Fabrication and mechanical properties of SiO<sub>2</sub> matrix composites reinforced by carbon nanotube, *Mater. Sci. Eng.: A.* 357 (2003) 392-396.
- [10] Y. Yang, M.C. Gupta, K.L. Dudley, Studies on electromagnetic interference shielding characteristics of metal nanoparticle-and carbon nanostructure-filled polymer composites in the Ku-band frequency, *Micro. Nano Lett.* 2 (2007) 85-89.
- [11] C. Hai, T. Shirai, M. Fuji, Fabrication of conductive porous alumina (CPA) structurally modified with carbon nanotubes (CNT), *Adv. Powder Technol.* 24(2013), 824-828.
- [12] W. Li, X. Wang, Z. Chen, M. Waje, Y. Yan, Carbon nanotube film by filtration as cathode catalyst support for proton-exchange membrane fuel cell, *Langmuir.* 21 (2005) 9386-9389.
- [14] A. Chaipanich, T. Nochaiya, W. Wongkeo, P. Torkittikul, Compressive strength and microstructure of carbon nanotubes-fly ash cement composites, *Mater. Sci. Eng. A.* 527 (2010) 1063-1067.
- [13] Y.S. Tang, J.Kong, J.W. Gu, G.Z. Liang, Reinforced cyanate ester resins with carbon nanotubes: surface modification, reaction activity and mechanical properties analyses, *Polym-plast. Technol.* 48 (2009) 359-366.
- [15] E. Kymakis, I. Alexandou, G.A.J. Amaratunga, Single-walled carbon nanotube-polymer composites: electrical, optical and structural investigation,

- Synthetic Metals. 127 (2005) 59-62.
- [16] J. Heidarian, A. Hassan, R.A. Lafia-Araga, Improving the thermal properties of fluoroelastomer (Viton GF-600S) using carbon nanotube, *Compos. Interface.* 23 (2016) 191-207.
- [17] L. Sun, H. Cai, W. Zhang, X. Ren, P. zhang, Preparation and electrochemical performance of Cu<sub>6</sub>Sn<sub>5</sub>/CNTs anode materials for lithium-ion batteries, *Integr Ferroelectr.* 171 (2016) 193-202.
- [18] S.B. Sinnott, Chemical functionalization of carbon nanotubes, *J. Nanosci. Nanotechnol.* 2 (2002) 113-123.
- [19] W.M. Daoush, B.K. Lim, C.B. Mo, D.H. Nam, Electrical and mechanical properties of carbon nanotube reinforced copper nanocomposites fabricated by electroless deposition process, *Mater. Sci. Eng. A.* 513 (2009) 247-253.
- [20] M. Zhang, L. Su, L. Mao, Surfactant functionalization of carbon nanotubes (CNTs) for layer-by-layer assembling of CNT multi-layer films and fabrication of gold nanoparticle/CNT nanohybrid, *Carbon.* 44 (2006) 276-283.
- [21] X. Yang, E. Liu, C. Shi, J. Li, N. Zhao, Fabrication of carbon nanotube reinforced Al composites with well-balanced strength and ductility, *J. Alloy. Compd.* 563 (2013) 216-220.
- [22] A.K. Bledzki, J. Gassan. Composites reinforced with cellulose based fibres, *Prog. Polym. Sci.* 24 (1999) 221-274.
- [23] M. Mukherjee, G. Nayak, S. Bose, C.K. Das, Improvement of the properties of PC/LCP/MWCNT with or without silane coupling agents, *Polym-Plast. Technol.* 48 (2009) 1107-1112.
- [24] A. Hirsch, Functionalization of single-walled carbon nanotubes, *Angew. Chem.*

- Int. Edit.. 41 (2002) 1853-1859.
- [25] J.N. Coleman, U. Khan, W.J. Blau, Y.K. Gun'ko, Small but strong: a review of the mechanical properties of carbon nanotube-polymer composites, *Carbon*. 44 (2006) 1624-1652.
- [26] P.C. Ma, J.K. Kim, B.Z. Tang, Effects of silane functionalization on the properties of carbon nanotube/epoxy nanocomposites, *Compos. Sci. Technol.* 67 (2007) 2965-2972.
- [27] P.M. Vitousek, H.A. Mooney, J. Lubchenco, J.M. Melillo, Human domination of Earth's ecosystems, *Science*. 277 (1997) 494-499.
- [28] S.L. Shi, J. Liang, The effect of multi-wall carbon nanotubes on electro magnetic interference shielding of ceramic composites, *Nanotechnology*. 19 (2008) 5707.
- [29] T.T.T. Hien, T. Shirai, M. Fuji. An advanced fabrication route for alkali silicate glass by non-firing process. *Adv. Powder Technol.* 25 (2014) 360-364.
- [30] E.U. Apiluck, T. Shirai, K. Tomoaki. H. Watanabe, M. Fuji, M. Takahashi, Novel fabrication route for porous ceramics using waste materials by non-firing process, *J. Ceram. Soc. Jpn.* 1380 (2010) 745-748.
- [31] G. Gorrasi, A. Sorrentino, Mechanical milling as a technology to produce structural and functional bio-nanocomposites, *Green Chem.* 17 (2015) 2610-2625.
- [32] T. Shirai, K. Orito, T.T.T. Hien, M. Fuji, Effects of different forming methods on the properties of solidified body by non-firing process through the mechanochemical treatment, *J. Jpn. Soc. Powder. Powder. Met.* 59 (2012) 517-521.

- [33] S.C. Velasco, H.A.L. Martinez, C.M. Lozada, C.A. Alvarez, V.M. Castano, Chemical functionalization of carbon nanotubes through an organosilane, *Nanotechnology*. 13 (2002) 495.
- [34] L. Valentini, J. Macan, I. Armentano, F. Mengoni, J.M. Kenny, Modification of fluorinated single-walled carbon nanotubes with aminosilane molecules, *Carbon*. 44 (2006) 2196-2201.
- [35] M. Lavorgna, V. Romeo, A. Martone, M. Zarrelli, M. Giordano, G.G. Buonocore, M.Z. Qu, G.X. Fei, H.S. Xia, Silanization and silica enrichment of multiwalled carbon nanotubes: Synergistic effects on the thermal-mechanical properties of epoxy nanocomposites, *Eur. Polym. J.*. 49 (2013) 428-438.
- [36] Y.N. Pozhidaev, O.V. Lebedeva, Hybrid composites based on 3-aminopropyltriethoxysilane and nitrogen polybases, *Russ. J. Appl. Chem.*. 85 (2012) 244-247.
- [37] M.S. Dresselhaus, G. Dresselhaus, A. Jorio, A.G. Souza Filho, R. Saito, Raman spectroscopy on isolated single wall carbon nanotubes, *Carbon*. 40 (2002) 2043-2061.
- [38] S.M. Yuen, C.C.M. Ma, C.L. Chiang, C.C. Teng, Morphology and properties of aminosilane grafted MWCNT/polyimide nanocomposites, *J. Nanomater.*. 2008 (2008) 4.
- [39] Q. He, T. Yuan, X. Yan, D. Ding, Q. Wang, Z. Luo, Flame-Retardant Polypropylene/Multiwall Carbon Nanotube Nanocomposites: Effects of Surface Functionalization and Surfactant Molecular Weight. *Macromol. Chem. Phys.*. 215 (2014) 327-340.
- [40] S. Contarini, S.P. Howlett, C. Rizzo, B.A. De Angelis, XPS study on the

dispersion of carbon additives in silicon carbide powders. *Appl. Surf. Sci.* 51  
(1991) 177-183.

## **Chapter6 General Conclusion**

In order to fabricate carbon doped functional material with high dispersibility, electrical conductivity, as well as mechanical property, this thesis focused on two dimensionality of carbon filled material: carbon nanoparticles/polymer 2D membrane, carbon nanoparticles/silica 3D ceramic bulk material and carbon nanotubes/silica 3D ceramic bulk material. This study investigated the possibility of carbon materials connected to each other in the matrix material to form a complete path, providing conductivity to the matrix material. In the case of ensuring the structure of the composite, more application possibilities are provided for the base material, which have relatively lower functionality.

In Chapter 2, a kind of 2D material, electro-conductive membranes, formed by carbon nanoparticle network array were fabricated via micro-phase separation process in the polymer system of cellulose acetate/acetone/water ternary solution. Micro-phase separation technique is the most common method for preparation and production of polymeric membrane. With the formation of polymer network, added nanoparticles became network by the drive of non-solvent owing to thermodynamic and compatible properties between particles and ternary solution. Meanwhile, the nanoparticle surface properties affected the binding force of neighbor particles for the continuous nanoparticle network structure. Heat treatment on the membrane aims at removing polymer from. Thus, electro-conductive nanoparticle network membrane can be facilely prepared.

In Chapter 3, carbon nanoparticle/silica 3D ceramic composite matrix was fabricated by non-firing process. To determine the relationship of carbon filler amount

and the physical properties including electro-resistivity and mechano-property, different volume percentage of carbon nanoparticles were added into base silica ceramic of different carbon ratios. Results show that the carbon nanoparticles/silica solidified body percolates with 40 vol.% of filler. Also, from the results of three-point bending test, the highest strength was at 20% of carbon nanoparticles. At this time, the strength was highest by preventing shrinkage as aggregate by carbon nanoparticles and making internal stress less likely to influence mechanical property. However, when increasing the amount of carbon nanoparticles to percolation concentration, the bond between silica was broken and the strength decreased.

In Chapter 4, to improve the silica ceramic composite property by using another kind of carbon filler structure (carbon nanoparticles to carbon nanotubes), CNTs/silica ceramic composite with electro-conductivity was fabricated and its application on electromagnetic field was also discussed. Carbon composite ceramics have much attention for industry because of their excellent properties such as strong toughness, high electrical conductivity as well as low percolation threshold. Therefore, carbon nanotubes (CNTs) were used to incorporate with silica ceramics in order to improve their electromagnetic properties. The amount of CNTs in CNTs/silica composite ceramics was varied in order to investigate its effect on morphologies and electromagnetic properties of those. The composites were successfully fabricated by non-firing process. The results revealed that the obtained CNTs/silica composite ceramic have an electrical resistivity of  $66.6 \Omega \cdot \text{cm}$  with a bending strength of 13.8 MPa. At the same time, the electromagnetic wave reflective ability achieved 70% over a wide frequency. This indicates that the CNTs in CNTs/silica composite ceramics may be potentially applied for an electromagnetic wave reflective material.

Chapter 5 introduced that CNTs/ceramic composites have much attention for the industry because of their excellent properties. The interfacial bonding of silane functionalized multi-walled carbon nanotubes adding silica ceramic composites by a non-firing process was investigated in this work. MW-CNTs were previously oxidation treated by mixed acid for the further surface modify with the participation of a silane 3-aminopropyl triethoxysilane (APTES), which improves the chemical bonding and dispersibility of CNTs in ceramic bodies. The extent of APTES chemical functionalization and mechanical property of CNTs/silica ceramic composites were investigated. Results showed that composites were facily prepared without calcining or sintering to form ceramic materials, and also showed that oxidization treatment introduced functional groups to CNTs surface for stable interfacial reacting with the amino groups on APTES. Obtained APTES-CNTs was sequentially combined with surface activated silica. This finding confirmed the improvements of dispersibility and enhanced mechanical property of composite material successfully.

Based on the above mentioned studies, it can be concluded that our study focused on investigating the ability of carbon materials filled different dimensionality (2D and 3D) functional nanocomposites prepared by phase-separation process and an environmental friendly ceramic material fabrication method named non-firing process to be applied as electrical and EMI shielding materials. Different kinds of carbon materials having excellent conductive properties are added to the membrane polymer material and the bulk ceramic material so that the insulating material has electrical conductivity. The dispersibility and percolation threshold of carbon materials in the matrix materials were studied and finally applied to conductive composite materials and electromagnetic shielding materials. In recent years, most researchers believe that

carbon nanotube-reinforced ceramic materials mainly depend on the dispersion of carbon nanotubes in the matrix, sufficient densification, and proper interfacial bonding between the carbon nanotubes and the matrix. In addition, it is also related to the amount of carbon nanotubes added and the structural integrity. Thus, There is still much work to do to improve this research in the future works: 1) Continuing to study the dispersion, interface and structural alteration of carbon materials in ceramics is still the focus of future research; 2) In order to improve the interface between carbon material and the matrix, designing and controlling the surface structure of carbon material through surface modification and multi-functionalization of carbon material are the main research directions in the future; 3) Improve the process route and study the appearance of CNTs/ceramic composite structures with strong mechanical properties. In addition, many scholars are currently systematically studying the effects of carbon material size, purity, defects, electron theory, heat conduction, process improvement, and composite material interface bonding strength on performance.

## Research Activities

1. (Poster presentation) **Peng Bo**, Takai Chika, Takashi Shirai, Fuji Masayoshi.  
Preparation and Characterization of Nanoparticles Network Formed by  
Micro-phase  
Separation.  
The 48th Association of Tokai Young Ceramists, Mie, Japan, Jun. 26-27, 2014
2. (Oral presentation) **Peng Bo**, Takai Chika, Takashi Shirai, Fuji Masayoshi.  
Synthesis of Functional Nanoparticles Network Membrane via Micro-phase  
Separation.  
The 52<sup>nd</sup> Symposium on Powder Science and Technology, Himeji, Japan, Sept.  
25-27, 2014
3. (Oral presentation) **Peng Bo**, Takai Chika, Takashi Shirai, Fuji Masayoshi.  
Synthesis of Silver Nanoparticles Network Membrane by a Micro-phase  
Separation Process.  
The 53<sup>rd</sup> Symposium on Basic Science of Ceramics, Kyoto, Japan, Jan. 8-9, 2015
4. (Oral presentation) **Peng Bo**, Takai Chika, Takashi Shirai, Fuji Masayoshi.  
Fabrication of Nanoparticle Functional Network Membrane by the Micro-phase  
Separation Process.  
The 5th International Conference on the Characterization and Control of Interfaces  
(ICCCI) for High Quality Advanced Materials and the 51st Summer Symposium  
on Powder Technology, Kurashiki, Japan, July 7-10, 2015
5. (Oral presentation) **Peng Bo**, Takai Chika, Takashi Shirai, Fuji Masayoshi.  
Fabrication of Nanoparticle Functional Network Membrane by the Micro-phase

Separation Process.

The 1st Joint Students Seminar of BUCT and NIT, Beijing, China, Oct. 27-30, 2015

6. (Poster presentation) **Peng Bo**, Takai Chika, Takashi Shirai, Fuji Masayoshi.  
Fabrication of Functional Non-firing Ceramics through Mechano-chemical Treatment.  
The 52th Association of Tokai Young Ceramists, Gifu, Japan, Jun. 23-24, 2016
7. (Oral presentation) **Peng Bo**, Takai Chika, Takashi Shirai, Fuji Masayoshi.  
Fabrication of Nanoparticle Functional Network Membrane by the Micro-phase Separation Process.  
2016 International Symposium on Integrated Molecular/Materials Science & Engineering (IMSE 2016), Qingdao, China, Oct. 13-16, 2016
8. (Oral presentation) **Peng Bo**, Goto Satono, Razavi-Khosroshahi Hadi, Takai Chika, Fuji Masayoshi.  
A Facile Way to Fabricate Carbon-Ceramic Nanocomposites Through a Mechano-chemical Treatment Without Sintering Process  
12th Pacific Rim Conference on Ceramic and Glass Technology (PACRIM 12), including Glass & Optical Materials Division Meeting (GOMD 2017), Hawaii, America, May 21-26, 2017.
9. (Oral presentation) **Peng Bo**, Takai Chika, Razavi-Khosroshahi Hadi, Fuji Masayoshi.  
Fabrication of Functional Ceramics Through a Non-firing Process and Its Electromagnetic Property  
Spring Meeting of the Japan Society of Powder and Powder Metallurgy, 2017.

Tokyo, Japan, May 31-Jun. 2, 2017

10. (Oral presentation) **Peng Bo**, Takai Chika, Razavi-Khosroshahi Hadi, Fuji Masayoshi.

Facile and Energy-saving Way to Fabricate Functional Carbon-Ceramic Nanocomposites Without Sintering Process

Seminar of Phenomena Related to Powder Materials, Nara, Japan, Aug. 7-9, 2017.

11. (Oral presentation) **Peng Bo**, Takai Chika, Razavi-Khosroshahi Hadi, Fuji Masayoshi.

Processing and Properties of Silica Based Carbon-ceramic Nanocomposites Fabricated by a Facile and Environmental Friendly Method

International Conference on Powder and Powder Metallurgy, Kyoto, Japan, Nov. 6-9, 2017.



## List of Publications

1. **Peng Bo**, Takai Chika, Fuji Masayoshi, Takashi Shirai, Formation of nanoparticle added functional polymer network membrane via micro-phase separation process, *Advanced Powder Technology*, 27 (3)(2016) 871-876.
2. **Peng Bo**, Takai Chika, Hadi Razavi-Khosroshahi, Montaser Sabbah El Din EL Salmawy, Fuji Masayoshi, Effect of CNTs on morphology and electromagnetic properties of non-firing CNTs/silica composite ceramics, *Advanced Powder Technology*. (DOI: 10.1016/j.apr.2018.04.024).
3. **Peng Bo**, Takai Chika, Hadi Razavi-Khosroshahi, Fuji Masayoshi, Effect of silane modification on CNTs/silica composites fabricated by a non-firing process to enhance interfacial property and dispersibility, *Advanced Powder Technology*. (DOI: 10.1016/j.apr.2018.05.017).



## **Acknowledgement**

I would like to thank my supervisor Prof. Masayoshi Fuji gratefully for his selfless, kind, and patient supervision and suggestions of not only the professional knowledge and academic experience, but also the way of thinking about and solving problems. I would also like to thank Prof. Takashi Shirai, Dr. Chika Takai, Dr. Razavi Hadi, Dr. Walaiporn Suthabanditpong, other professors and members of the Advanced Ceramics Research Center, for their kind guidance and helps. I acknowledge Prof. Wang Feng in State Key Laboratory of Chemical Resource Engineering, Beijing Key Laboratory of Electrochemical Process and Technology for Materials, Beijing University of Chemical Technology. Last but not the least, Additionally, I would like to express my gratitude to my family and close friends for their years of support.